Characterization of uranium mined ore for nuclear forensic applications

Liteboho Ntsohi

A dissertation submitted to the Faculty of Science, University of the Witwatersrand, Johannesburg,
in fulfilment of the requirements for the degree of
Master of Science.

2019

Supervisor: Dr. Iyabo Usman (University of Witwatersrand)
Co-supervisor: Dr. Risimati Mavunda (NECSA)

Declaration

I declare that this dissertation is my own, unaided work. It is being submitted for the Degree of Master of Science at the University of the Witwatersrand, Johannesburg. It has not been submitted before for any degree or examination at any other University.

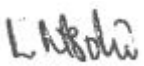

13 June 2019

Abstract

Nuclear forensic science aims to find signature of nuclear or radioactive material that can aid with the attribution process. Uranium compounds have isotopic or chemical characteristics that provide specific information concerning their origin and production process. Examples of such signatures are uranium and thorium isotopic and activity concentration, trace element content, rare earth elements, among others. This dissertation investigated the applicability of these signatures in environmental samples from uranium mining areas in Nigeria and Botswana using Inductively Coupled Plasma Mass Spectrometer (ICP-MS) and X-Ray Fluorescence (XRF), techniques. In this study uranium ore samples from five mining regions in Nigeria (Riruwai, Mika 1, Mika 2, Michika) and in Botswana (Serule) were analyzed to determine the isotopic and elemental signatures for the regions. The Uranium and Thorium isotopic and activity concentrations for these areas were compared to determined the significance of the signatures in these regions. From the obtained data, both rare earth elements and impurity elements were determined and subjected to ANOVA in order to quantify their statistical significance in the observed variations. For Nigeria samples, the results confirm that REE and impurity element patterns used for origin location exhibit significant variation within the considered mine areas. However, this variation can not be deduced from the Botswana samples despite further mineralogy analysis with XRF.

Dedication

To my angels

Acknowledgements

I wish to thank most deeply my supervisor, Dr Iyabo Usman, who provided, without hesitation, constructive comments, suggestions and criticism, all of which provided a strong backing for this Masters research work. My co-supervisor, and Dr Rasimiti Mavunda, who steered me in the right direction whenever it was necessary, I am indebted to his valuable comments on this dissertation.

I wish to express my deepest gratitude to Miss Mokgaetji Monyai and Mr Marlin Patchappa who, without hesitation helped with the ICP-MS and XRF measurements. This research would have not been possible without your expert imput.

I give thanks to my friends; Lintle Phakisi, Nyakallo Matlali, Palesa Rapapa and Tsepiso Pulumo and siblings; Motsamai, Mamohale, Makay, Nthati, Linono and Litsitso for the constant support and encouragement they provided to me during my difficult and trying times in the course of this study.

Finally, my most sincere gratitude goes to my parents; Dr. 'Mamosa Nts'ohi and Col. Tau Nts'ohi, whose loving guidance provided me with unfailing support and encouragement through this process. For having made the journey less bumpy, I am very grateful.

Contents

Declaration ii

Abstract iii

Dedication iv

Acknowledgements v

List of Figures ix

List of Tables x

1 Introduction 1

2 Literature Review 9

2.1 Radioactive decay 9

2.1.1 Alpha (α) decay 10

2.1.2 Beta (β) decay 10

2.1.3 Gamma decay 11

2.1.4 Radioactive Decay rates 12

2.2 Naturally Occurring Radioactive Materials 14

2.3 Nuclear fuel cycle 16

2.3.1 Uranium mining 18

2.3.2 Uranium Milling Process 18

2.3.3 Uranium Conversion Process 19

2.3.4 Uranium Enrichment Process 19

2.3.5 Fuel fabrication 21

2.4 Uranium mining in Africa 22

2.4.1 Botswana 24

2.4.2 Nigeria 24

2.5 Characteristic parameters of uranium bearing materials 26

2.5.1 Isotopic patterns in uranium deposits 27
2.5.2 Uranium chronometry 28
2.5.3 Isotopic composition of Stable isotopes 29
2.5.4 Impurities and trace elements 31
2.5.5 Minerology 33

3 Methodology **34**
3.1 Sequencing of techniques 34
3.2 Applied Measurement techniques 35
3.2.1 Inductively Coupled Plasma Mass Spectrometry (ICP-MS) 36
3.2.2 X-Ray Fluorescence 39
3.2.3 Limitations and merits of XRF over ICP-MS 43
3.3 Experimental procedure 44
3.3.1 Samples chosen for the study 44
3.3.2 Sample collection 46
3.3.3 Sample preparation 47
3.4 Experimental technique 48
3.4.1 Measurement using ICP-MS 48
3.5 Method of Analysis 50

4 Data Analysis, Results and Discussion **53**
4.1 Characterization of uranium mined samples 54
4.1.1 Uranium and Thorium composition in the samples . . . 54
4.1.2 Activity concentration of uranium samples 58
4.1.3 Activity ratio of Uranium samples 63
4.1.4 Rare Earth Elements 65
4.1.5 Impurity Elements 69
4.2 Statistical Analysis of result 71
4.2.1 Results of ANOVA analysis on Rare Earth Elements (REE) 72
4.2.2 Results of ANOVA analysis on Impurity elements 73
4.3 Mineral identification and quantification 74

5 Conclusion and Recommendations **75**
5.1 Recommendations 76

List of Figures

2.1 Schematic representation of the ^{232}Th series (taken from Ref. [Swi15]) 15
2.2 Schematic representation of the ^{238}U series (taken from Ref. [Swi15]) 16
2.3 Schematic representation of the ^{235}U series (taken from Ref. [Swi15]) 16
2.4 Flow chart representation of the nuclear fuel cycle (taken from Ref. [Kri16]) 17
2.5 Schematic representation of the gaseous diffusion process (taken from Ref. [Com17]) 20
2.6 Schematic diagram illustrating a basic centrifugal enrichment process (taken from Ref. [Com17] 21
2.7 Schematic chart of the uranium reconversion process in the nuclear fuel cycle (taken from Ref. [Age09]) 22
2.8 Map showing the locations of uranium deposits in Africa. The areas marked with yellow circles show primary deposits, where uranium occurs as the main commodity. The red squares mark secondary deposits, where uranium is a by-product (taken from Ref. [Das12]) 23
2.9 Illustration of valid nuclear forensic signatures and the domain of possible material that match those material signatures (taken from Ref. [Gue13]) 26

3.1 Inductively Coupled Plasma-Mass Spectroscopy instruments (taken from Ref. [Bor13].) 37
3.2 A schematic diagram of Quadrupole Inductively Coupled Plasma-Mass Spectroscopy components (taken from Ref. [Bor13]) 38

3.3 A schematic diagram of the Bohr model of an atom. The L-shell electrons are dropping to lower energy levels to replace the lost K-shell electrons, causing a release of photons in the X-ray spectrum. Similarly, M-shell electrons are dropping energy levels to replace the electrons lost by the L-shell. Each transition produces a photon of quantized energy which is measured by XRF (taken from Ref. [Bou14]) 41
3.4 Map of Nigeria showing showing sampling regions 45
3.5 Map of Botswana showing Serule (yellow dot) where samples were collected (taken from Ref. [con19]) 46
3.6 Grinding machine and milling machine used in sample preparation 47
3.7 Transformational steps in sample preparation 48
3.8 Microwave system used for sample preparation 49
3.9 A section of F-Table used to determine the F-critical used in ANOVA (taken from Ref. [fta19]) 52

4.1 Calibration of ICP-MS device with standards for ^{232}Th, ^{238}U radionuclides 54
4.2 ^{232}Th, ^{238}U and ^{235}U isotopic concentration in the samples . . . 56
4.3 ^{232}Th, ^{238}U and ^{235}U activity concentration in the samples . . . 61
4.4 REE concentration for S1,S2, S3 and S4 obtained from ICP-MS analysis of results 65
4.5 Bar charts of REE concentrations for S1, S2, S3, S4 as observed from ICP-MS measurements 66
4.6 REE concentration for S5, S6, S7, S8 and S9 obtained from ICP-MS analysis of results 67
4.7 Bar charts of REE concentrations for S5, S6, S7, S8, and S9 as observed from ICP-MS measurements 68
4.8 Normalized REE for all samples obtained from ICP-MS analysis of results 69
4.9 Bar charts of impurity elements concentration for S1, S2, S3, S4 as observed from ICP-MS measurements 70
4.10 Bar charts of impurity elements concentration for S5, S6, S7, S8 and S9 as observed from ICP-MS measurements 71

List of Tables

1.1 Nuclear forensic signatures that have been identified (taken from Ref. [Kri16]) 4

2.1 New uranium mining projects in Africa (taken from Ref.[Age18, Pro19]) 25

3.1 Analytical techniques that can be used to find information on Uranium-bearing materials (taken from Refs. [Red09]) 35
3.2 Origin of the samples under investigation 44

4.1 Isotopic concentrations of ^{232}Th, ^{238}U and ^{235}U in the measured samples including their uncertainties. 55
4.2 Activity concentrations of ^{232}Th, ^{238}U and ^{235}U in the measured samples including their uncertainties 60
4.3 Activity concentration ratios ^{232}Th/^{238}U and ^{235}U/^{238}U in the measured samples 63
4.4 REE F-statistics for S1, S2, S3 and S4 samples 72
4.5 Impurity element F-statistics for S1, S2, S3, S4 samples. 73
4.6 Major minerals in S5, S6, S7, S8 and S9 74

Chapter 1

Introduction

Background

For the past three decades, nuclear forensic science has become an essential element of the nuclear security strategy [Kee16]. The idea that certain characteristics of a material are inherent and could be used to trace the origin of any seized nuclear material was developed in response to large number of seizures involving plutonium and highly enriched uranium in an attempt to thwart nuclear smuggling [Hut15, Vér10].

Following the dissolution of the Soviet Union in the early 1990s, a large number of nuclear manufacturing and research facilities were shut down [Kri16]. Nuclear arsenal from these facilities were relocated to Russia, Belarus, Ukraine and Kazakhstan [Moo14]. During this period, large amounts of nuclear and other radioactive materials were lost, creating a problem of orphan sources [Kee16]. Also, most of the relocation facilities did not have sufficient safe guards in place to prevent theft of the material [Moo14].

Poor physical security, inadequate material protection measures, lack of control and accountability were the norm at the sites regardless of the nature of materials being handled [Fed15]. During this time, Europe saw an increase in seizures involving nuclear and other radioactive material at international borders[Wal06]. This marked the beginning of a new security threat termed "nuclear smuggling".

The first incidents of nuclear smuggling were reported in 1991 in Italy, Switzerland and Soviet Union. Later more cases were reported in Germany,

Czech Republic, Hungary and other central European countries [Khu18]. Since then law enforcement agencies have seized several Special Nuclear Material (SNM) and intercepted sales of non SNM radioactive materials though out Europe [Moo14]. Until 1991, all intercepted black market trades were scams, but between 1991-1994 legitimate cases involving SNM emerged on the black market, proving that weapon usable nuclear material was indeed available on the black market. In response to this availability, the global community has focused its attention on ways to counter the threat [Kra14]. Developing new innovative disposal procedures for dismantlement operations improved nuclear safeguard. This reduced diversion of the nuclear material from regulatory control. In order to keep record of smuggling incident, a database was created. Most importantly, a new scientific field was also developed and has since become a global priority [Kee16, May07, Moo14].

An Incident and Trafficking Database (ITDB) was established in 1995 by the International Atomic Energy Agency to record and analyze incidents where nuclear and other radioactive materials were found out of regulatory control [Iaea17, Rea16]. By 31 December 2016, the database contained 3068 incidents reported, of which 270 were confirmed acts of trafficking or malicious use [Iaea17, Rea16]. These numbers created a serious concern and need for nuclear laboratories to develop rapid, effective tools for identification of origin of nuclear or other radioactive materials found out of regulatory control (MORC) [Kea15].

Following seizures involving nuclear and other radioactive materials, law enforcement agencies were left with a number of questions. These include: what was the material?, where does it originate?, who was its last legal owner?, what was the smuggling route?, and what was the intended use of the material? [Kee16, May07, Agg16]. Nuclear forensic science was thus developed to provide answers to these questions [Hut15, L'An12].

Essentially, nuclear forensic science is a technical means by which nuclear material or radioactive material, whether intercepted intact, or retrieved from post-explosive debris, are characterized (as to determine composition, physical condition,age, provenance, history). The results are then interpreted through the use of analytic techniques from nuclear safeguards, chemistry and physics [Kri11, Gue13, Fed15].

Nuclear forensic analysis involves an iterative approach in which results from one analysis serve as a guide to subsequent analysis [Kea15]. There are three levels of analysis - categorization, characterization and full nuclear forensic analysis. Categorization aims to find the bulk constituents in order to determine the threat level posed by the material [Kri11]. It occurs on-site and utilizes non-destructive analytical tools. This analysis distinguishes between naturally occuring radioactive material (NORM), SNM, radioactive contamination and commercial radioactive sources [Kea15]. Characterization determines the nature of evidence. It provides a full elemental analysis of the material; major, minor and trace constituents as well as determination of the isotopic properties [Kri11]. The aim of full nuclear forensic analysis is to analyze all radioactive and traditional evidence to address questions on origin, production method, loss of legal control and the likelihood of more being available. A detailed interpretation includes comparison of measured signatures against information contained in a nuclear forensic database/library [Kea15]. This is an important part of the attribution process.

A nuclear forensic library is a national database system for identification of nuclear and other radioactive materials found out of regulatory control. The database contains information on nuclear and other radioactive material produced, used and stored in the state. It enables comparison of analytical results of material found out of regulatory control to analytical information of known material to help in source attribution. Countries have incorporated nuclear forensic science as part of their strategy to prevent and respond to nuclear incidents [Agg16]. Attribution process employs four main inputs [Kri04, L'An12];

- results from nuclear forensic analysis of samples;
- understanding of radio-chemical and environmental signatures;
- knowledge of production methods used for nuclear material and the development pathways;
- information from law enforcement and intelligence sources.

It is the integration of all forms of information about a nuclear incident into data that can be easily analyzed and interpreted to form the basis of confident response to the incident [L'An12] .

There are three ways to apply Nuclear forensics as described by Ian D Hutcheon [Hut15, Gue13] point-to-population comparison, which connects a sample to a known population of a materials, such as uranium oxide from a particular mine; point-to-point comparison, which is used when trying to match sample to a source; and finally point to model comparison, when data is not available or limited, this is used to explore possible origins of material under consideration [Hut15, Gue13].

Conventional forensic science has long been applied in criminal investigations [Mal09]. The analysis of human finger and palm print has become a valuable investigative technique [Mal09, L'An12]. It is fundamentally an application of pattern recognition, where the print ridge characteristics of specimen in question is compared to those within a database [Mal09, L'An12]. Over the last three decades, another technique based on genetic variation termed DNA was developed and has also proven valuable in forensic science [L'An12]. In the same fashion as conventional forensics, nuclear forensics relies on the fact that certain measurable parameters in a material are characteristic to the given sample [L'An12]. An unknown material may be characterized by measuring a set of those parameters to establish the so-called "nuclear fingerprint". Using this fingerprint, one can draw conclusions on the origin and intended use of the material [May13].

In order to build a nuclear fingerprint however, parameters that are determined by the raw material or fabrication process should be identified, only those are useful in attribution process [Hut15]. Over the years, several researches have been conducted globally and such parameters have been identified. Table 1.1 shows some of these parameters and the signatures they give.

Table 1.1: Nuclear forensic signatures that have been identified (taken from Ref. [Kri16])

Parameter	Signature
Appearance	Material type
U, Pu, content	Chemical concentration
Isotopic composition	Enrichment
Impurities	Geolocation
Age	Production date
Surface roughness	Production plant
Microstructure	Production process

In an effort to develop and enhance global nuclear forensic capabilities the five key issues affecting this development of nuclear forensics have been identified as follows [Gue13]

- There are strong capabilities in nuclear forensics but the ability to interpret data is still in a developmental state;
- Expanded database with information on nuclear material around the world are needed;
- Greater understanding of how materials change as they undergo reprocessing, processing, and other processes is needed;
- No single material provides the needed information for all, or even any material;
- Nonproliferation nuclear forensics requires a focused international cooperative effort.

The development of nuclear forensic capabilities in laboratories such as Lawrence Livermore National Laboratories (USA), Institute for Trans-uranium elements (Germany) and the International Technical Working group have created opportunities where global countries participate in the advancement of nuclear forensic abilities [Rea16]. To date, several signatures have been identified, however there is a gap in the information pertaining to African countries.

Problem statement

Extensive work is being conducted by the Livermore group to build a signature database/library, analyzing radioactive samples from several sources. The Lawrence Livermore team in the United States of America has developed a sourcing database and a database query system called Discriminant Analysis and Verification Engine (DAVE) [Agg16]. To date, their database has data points for more than 6,300 samples, from 133 sources in 31 countries, of yellow cake, uranium ore and uranium tetra-fluoride, all of which are in the early stages of the nuclear fuel cycle [Rea16]. The samples in the database are defined by 20 to 80 variables including major and minor trace element abundance and isotopic ratios[Agg16]. Although Lawrence Livermore group

has created a large database, there are samples from African countries that are not part of the database.

Even with these development and advancement of forensic knowledge, there is still a large gap in the field. Very little research has been conducted pertaining to African countries. Several countries in Africa have uranium deposits [Mat17]. Some countries such as South Africa, Namibia, Zambia and Tanzania have been actively mining uranium as a primary or secondary product [Das12]. South Africa has 71 uranium mines, Namibia has 42, Senegal, Tanzania and Zambia have 10, Botswana has 9 and Nigeria has 2 [Mat17]. These countries must observe the International Atomic Energy Agency (IAEA) Nonproliferation Treaty which aims at safeguarding nuclear and other radioactive material to prevent illicit trafficking. Countries should therefore have National Nuclear Programs aimed at the characterization of nuclear and other radioactive material found in and out of regulatory control [Joy11]. This characterization involves determination of chemical and isotopic concentration as well as physical parameters which form signatures of the origin. Currently there is no African country with a developed National Nuclear Library. Although South Africa has started, it does not possess a fully functional nuclear forensics laboratory [Mat17].

Objective

Methodology investigating the isotopic ratios $^{234}U/^{238}U$, $^{235}U/^{238}U$ and $^{236}U/^{238}U$ have been developed and validated as a fingerprint [Bre10, Kri16]. However, the $^{232}Th/^{238}U$ isotopic concentration ratio as well as the activity concentration ratio $^{232}Th/^{238}U$ have not. Using a limited number of signatures reduces the discriminating power for identifying origin of unknown nuclear materials, or for verifying processing at existing facilities [Sch18]. Nuclear forensic analysis generally advocates for the acquisition of large databases containing a variety of nuclear material signatures from a variety of analytical techniques [Sch18]. This study will measure and determine the $^{232}Th/^{238}U$ isotopic and activity ratios and investigates the potential use of these parameters as fingerprints.

The impurity spectrum of nuclear material displays the materials creation and production history, thus, can form a fingerprint [Gue13, May12]. During

processing steps of nuclear forensic cycle, different chemicals are introduced which alter the impurities [May12]. These chemicals create a signature and can be used to provide hints on the origin and production site [Gue13]. The impurity spectrum of the uranium mine ore therefore provides information on the geological origin and should be added to a library/database to be used as reference. The impurity spectrum of the regions under investigation will therefore be determined using Inductively Coupled Plasma-Mass Spectroscopy (ICP-MS) and its potential as a fingerprint will be determined using Analysis of Variance (ANOVA) statistical method.

This study focuses on West African region of Nigeria and South African region of Botswana which both have prospective uranium mining projects in the regions under investigation. The aim of this study is to analyse and characterize uranium mine ore from these two countries. The measured parameters will include the isotopic composition, concentration of the rear earth elements and the impurity spectrum. In addition to these parameters, the minerology of the samples from Botswana will be determined. The information and signatures found in this study can therefore be added to a National Nuclear Forensics Library and used as reference data to aid in source attribution of nuclear material found in and out of regulatory control.

Outline

The structure of this dissertation is as follows:

Chapter2 describes the theoretical background of this study. This includes the physical basis of Nuclear forensic analysis, Natural Occurring Radioactive Materials, the development of uranium mining in Africa and various signatures that have already been identified.

Chapter3 describes the experimental method used in nuclear forensic analysis and those which will be applied in this study. This includes the equipment used for analysis in this study and a detailed description of the experimental procedure followed.

Chapter4 outlines the analysis of the data procedure, presentation of the results obtained as well as a discussion of the results.

Chapter5 presents the conclusions of this study, as well as an overview of the proposed future work.

Chapter 2

Literature Review

Nuclear forensic analysis uses principles from physics, radiochemistry and nuclear safeguards to determine the origin of unattributed material. This chapter describes these concepts that form the basis for nuclear forensics and the methodologies that have been developed and validated in other studies.

2.1 Radioactive decay

Nucleus that are unstable decay in order to achieve neutron to proton (N:Z) ratio of the nearest possible stable nuclide [Mar12]. This process is often followed by the release of energy. Radioactive decay can therefore be defined as the spontaneous release of excess energy from unstable nucleus that results in the expulsion of particles or electromagnetic radiation [Rea16].

In 1897 Ernest Rutherford discovered that there was more than one type of radiation and each had a different degree of penetrating power [Rut10]. The less penetrating radiation emissions he termed alpha rays (α ray) and the more penetrating beta rays (β rays). It was observed that α and β rays could be deflected by a magnetic field and that the β particles had charge-to-mass ratio similar to that of the electron. After looking into the absorption properties of α particles, Marie Curie deduced that α particles were heavier particles [Mal11]. Rutherford successfully deflected α particles with a stronger magnetic field and later he and Royds proved that α particles were Helium nuclei [Eic18]. The charges of α particles and β particles were determined to be of opposite sign. A third type of radiation was discovered by Villard and he termed it gamma (γ) radiation. Unlike α and β rays, γ rays were not deflected by electric fields or magnetic fields and therefore carried no charge [Mar19].

2.1.1 Alpha (α) decay

Naturally occurring heavy nuclides with atomic number Z>74, and artificially produced transuranic elements with Z>82 undergo alpha decay (emission of a single alpha particle) [Mar12, Bry18]. Alpha decay is the spontaneous emission of a ^{4}He nucleus with 2 neutrons and 2 protons that results in physical changes in the parent isotope with atomic number Z and mass number A (^A_ZX) to produce a daughter isotope with atomic number Z-2 and mass number A-4 ($^{A-4}_{Z-2}Y$) [Vér10]. Although the kinetic energy of emission of α particles are high, the large mass of of the particle reduces the velocity to a few percent of the speed of light (c). Alpha particles are therefore non-relativistic. In comparison with other types of radioactive emissions, α emissions have a short range and can easily be stopped by a paper. Alpha particles are ejected with well defined energies that are characteristic of the emitting nuclei thus permitting spectroscopic measurements [Lil13]. Equation 2.1 shows a typical alpha decay in a nuclei.

$$^A_Z\mathrm{X} \rightarrow ^{A-4}_{Z-2}\mathrm{Y} + ^4_2\mathrm{He} + Q, \tag{2.1}$$

where X is a parent atom, Y is a daughter atoms and Q is the energy released. An example of α decay in nature is the decay of ^{238}U to ^{234}Th. Eq. 2.2 describes this process.

$$^{238}_{92}\mathrm{U} \rightarrow ^{234}_{90}\mathrm{Th} + ^4_2\mathrm{He} + Q. \tag{2.2}$$

2.1.2 Beta (β) decay

Similar to alpha decay, a parent isotope also undergoes physical changes to produce a new daughter isotope. The unstable parent nucleus emits a one electron (B^- decay) or a positron (B^+ decay) followed by a respective antineutrino ($\bar{\nu}$) or neutrino(ν) to become a more stable nucleus [Lil13, Rea16].

A neutron-rich nuclei generally undergoes β^- decay. This entails the emission of an electron at velocity close to the speed of light [Bry18, Eic18]. β^- decay is a consequence of the conversion of a neutron (n) into a proton (p) in the emitting nucleus and results in no change in the atomic mass number as

illustrated in Eq. 2.3 and Eq. 2.4:

$$ {}^{1}_{0}\mathrm{n} \rightarrow {}^{1}_{1}\mathrm{p} + {}^{0}_{-1}\beta + \bar{\nu}, \tag{2.3} $$

where n represents a neutron, p is a proton and $\bar{\nu}$ is an antineutrino.

The electrons emitted have energies ranging from Q-value to zero [Mar12, Lil13]. This is due to the conservation of lepton number which requires simultaneous emission of electrons and $\bar{\nu}$ for β^{-} decay.

$$ {}^{A}_{z}\mathrm{X} \rightarrow {}^{A}_{Z+1}\mathrm{Y} + {}^{0}_{-1}\beta + \bar{\nu}. \tag{2.4} $$

Equation 2.5 below shows an example of a β^{-} decay in thorium;

$$ {}^{234}_{90}\mathrm{Th} \rightarrow {}^{234}_{91}\mathrm{Pa} + {}^{0}_{-1}\mathrm{e} + \bar{\nu}. \tag{2.5} $$

Two other types of radioactive decay modes are classified under β decay: β^{+} decay and electron capture decay [Bry18]. Both types result in the conversion of a proton into a neutron without causing a change in the atomic mass. β^{+} decay is the emission of a positron while electron capture decay is one in which a nucleus captures atomic electron [Eic18, Lil13, Mar12]. Both processes are followed by emission of a neutrino.

2.1.3 Gamma decay

Following the alpha and beta decay processes, nuclei are often left in an excited state [Bry18, Mar12, Rea16]. To transition to a lower state, a nucleus dissipates energy. The transition energy δE, which is the energy difference between the initial state and the final states may appear in the form of a γ photon [Vér10]. Energy level occur at discrete energies and the γ rays from these transitions are emitted with well defined energies [Mar12, Lil13]. The energy of each photon emission is thus unique between parent and daughter states [Rea16]. Equation 2.6 describes a gamma decay in ^{238}U.

$$^{238}_{92}U \rightarrow ^{234}_{90} Th +^{4}_{2} He +^{0}_{0} \gamma \tag{2.6}$$

Internal conversion (IC) competes with γ emission in depopulating excited nuclear states [Moo14, Lil13]. This process occurs when external electromagnetic field of a nucleus interacts with atomic electrons such that energy and angular momentum are transferred to an electron, causing it to de-excite by ejecting an electron from one of the atomic orbits [Lil13]. IC and γ decay are both due to electromagnetic force.

2.1.4 Radioactive Decay rates

Radioactive elements undergo radioactive decay to attain stability. Radioactive decay can thus also be defined as the spontaneous transformation of an unstable parent nuclei into a more stable daughter nuclei until a stable daughter nuclei is reached. The probability per unit time that a given nucleus will undergo radioactive decay is called the decay constant (λ). For N radioactive nuclei in a sample, the rate of decay is given by Eq. 2.7 below.

$$\frac{dN}{dt} = -\lambda N. \tag{2.7}$$

The negative sign indicates that the number of atoms (N) decreases with time. Solving the differential Eq. 2.7 and imposing boundaries conditions $N = N_0$ at t = 0 we get the exponential law of radioactive decay shown in Eq. 2.8 ,

$$N_t = N_0 e^{-\lambda t}. \tag{2.8}$$

The intensity of radioactivity is called activity (A); this is a measure of disintegrations per unit time. Radio-chemists determined that the activity of a given prepared sample containing one radionuclide was proportional to the number of radioactive atoms (N) contained in the preparation [Eic18, Lil13]. This relationship is given by the fundamental law of radioactive decay shown in Eq. 2.9.

$$A = \lambda N. \tag{2.9}$$

The activity is measured in units of Becquerels (Bq), which is one disintegration per second.

Using Eq. 2.8 and Eq. 2.9 the activity can therefore be expressed as shown in Eq. 2.10;

$$A = \lambda N_0 e^{-\lambda t}. \tag{2.10}$$

.

The number of atoms present in a radioactive source is calculated using Eq. 2.11

$$N = \frac{M}{m} \times Av \tag{2.11}$$

.

where M is the weight of the radionuclide; m is the atomic mass of the radionuclide and Av is Avogadros number 6.02×10^{23} atoms per gram

The mean life τ of a radionuclide is the average lifetime of the radioactive nucleus. From Eq. 2.6, the number of nuclei which decay between time t and t + dt is given in Eq. 2.12;

$$dN = \lambda N dt = \lambda N(0) e^{-\lambda t} dt, \tag{2.12}$$

and

$$\tau = \frac{\int t dt}{\int dN} = \frac{1}{\lambda}. \tag{2.13}$$

The half life $t_{\frac{1}{2}}$ can be expressed in terms of either λ or τ as shown in Eq. 2.14:

$$t_{\frac{1}{2}} = \frac{In2}{\lambda} = \tau ln2. \tag{2.14}$$

Using Eq. 2.9 and Eq. 2.14, the activity can be expressed as shown in Eq. 2.15,

$$A = \lambda N = \frac{Nln2}{t_{\frac{1}{2}}} \tag{2.15}$$

The population of the daughter radionuclide depends on the decay constant of both the parent and the daughter [Vér10, Rea16]. This is because the daughter population grows according to the decay rate of the parent and decays according to its own decay rate. In cases where the decay rate and half life of the parent is significantly higher than that of the daughter, the two will fall into state of secular equilibrium [Vér10, Rea16]. At this state the quantity of radionuclides produced is equal to the rate at which it decays; such is the case when ^{238}U which has a significantly higher half life of 4.47 billion years as compared to its daughter ^{222}Rn.

Uranium bearing materials have been in the center of most smuggling incidents [Kri04]. Uranium is a naturally occurring radioactive materials (NORMS) that is essential in our everyday lives. It is the backbone of the nuclear power industry and military weapon programs worldwide [Moo14]. A single kilogram of highly enriched uranium (HEU) in the 1990s cost tens of thousands pounds to produce within a well established enrichment program [Moo14]. This put uranium in a unique position, thus making it a valuable commodity that is also highly vulnerable to smuggling.

2.2 Naturally Occurring Radioactive Materials

The components of the earth were created in a series of nuclear events. Beginning with the big bang, continuing quietly in the cores of burning stars, then rapidly in stellar explosions which distributed the product into space to be available for planet formation [Has14]. A lot of the nuclides formed were

radioactive. Most of them have however decayed away but a few with significantly longer half lives remain in varying quantities to date [Bae11]. Those nuclides constitute the bulk of the natural radioactivity in the environment. There are currently ten known naturally occurring radioelements with no stable isotopes found in the earths crust [Bae11]. These are Thorium, Uranium and elements generated from their decay. In addition to these, sixty radionuclides of elements that have stable isotopes also occur naturally. These are primordial nuclides (^{40}K, ^{87}Rb) or nuclides generated by impact of cosmic radiation (^{14}C, ^{3}H, ^{7}Be) or members of natural decay chains (^{210}Pb) [Ken09]. The earth bears a gross activity of about 10^{26} Bq, much greater man-made radioactivity. Naturally occurring radioelements are present at trace concentrations in material on earth at different concentrations and contributes to natural radioactivity of 24 $mSv/year$ [Has14].

There are three natural decay chains observed in nature: uranium series, actinium series, thorium series [Rea16]. Each of the series is headed by a long lived Parent; ^{238}U, ^{235}U and ^{232}Th. The nuclides in each series decay by emitting α particles and/or β particles until a final and stable nuclide is reached. Figure 2.1, Fig. 2.2 and Fig. 2.3 show the thorium series, uranium series and the actinium series respectively which are relevant to this work.

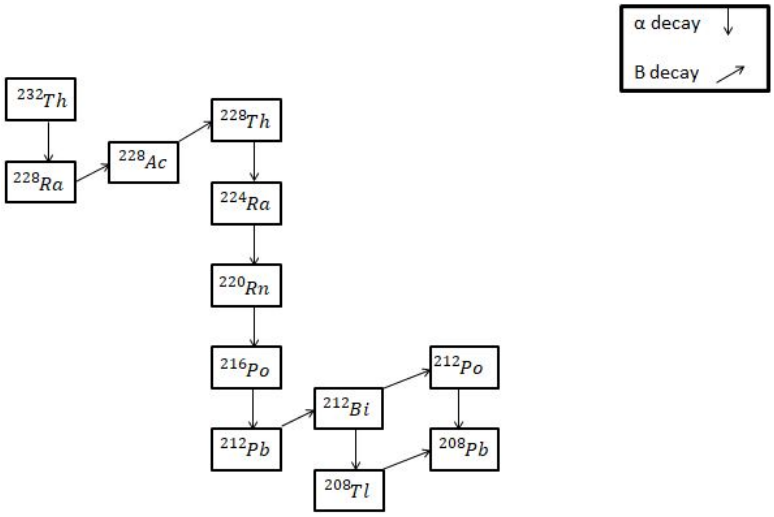

Figure 2.1: Schematic representation of the ^{232}Th series (taken from Ref. [Swi15])

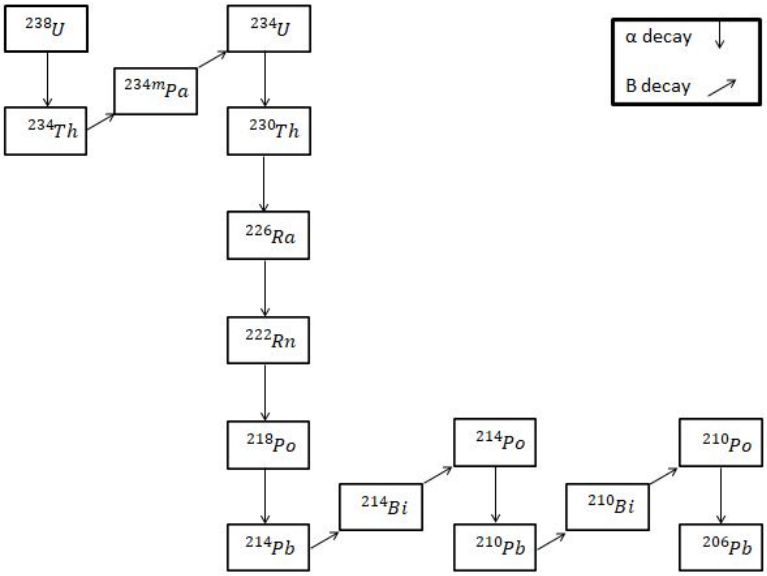

Figure 2.2: Schematic representation of the ^{238}U series (taken from Ref. [Swi15])

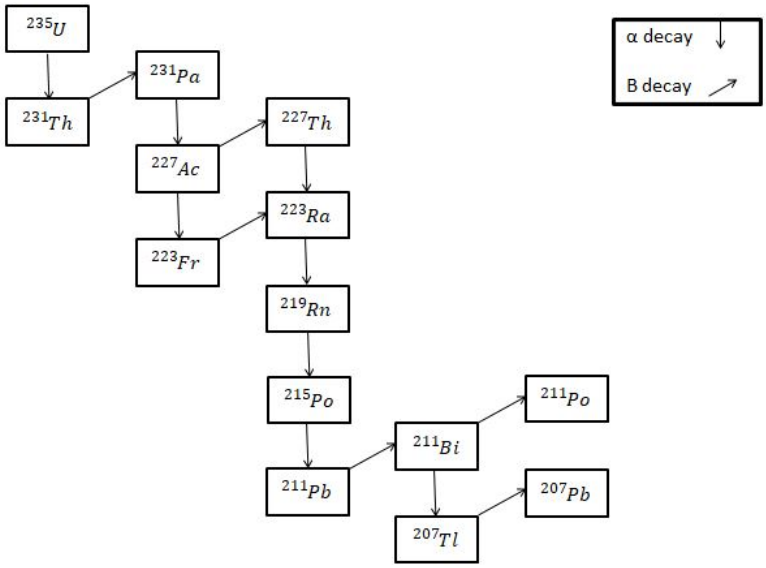

Figure 2.3: Schematic representation of the ^{235}U series (taken from Ref. [Swi15])

2.3 Nuclear fuel cycle

For uranium to be used as fuel, a sequence of processes and operations are necessary. These steps make up what is conventionally known as the nuclear

fuel cycle. In essence, the nuclear fuel cycle can be defined as a set of processes and operations necessary to manufacture nuclear fuel, its irradiation in nuclear power reactors and storage, reprocessing, recycling or disposal of irradiated fuel [Age09]. Beginning with mining of the ore and ending with the disposal of spent fuel and other forms of radioactive waste, this cycle describes the genesis of nuclear energy [Cro12]. The nuclear fuel cycle is divided into two major sections: the front end, which consists of mining, milling, conversion, enrichment and fabrication; and the back end, which is the temporary storage, reprocessing, recycling and ultimately waste disposal [Age09]. Figure 2.4 illustrates the sequences of processes in a typical nuclear fuel cycle.

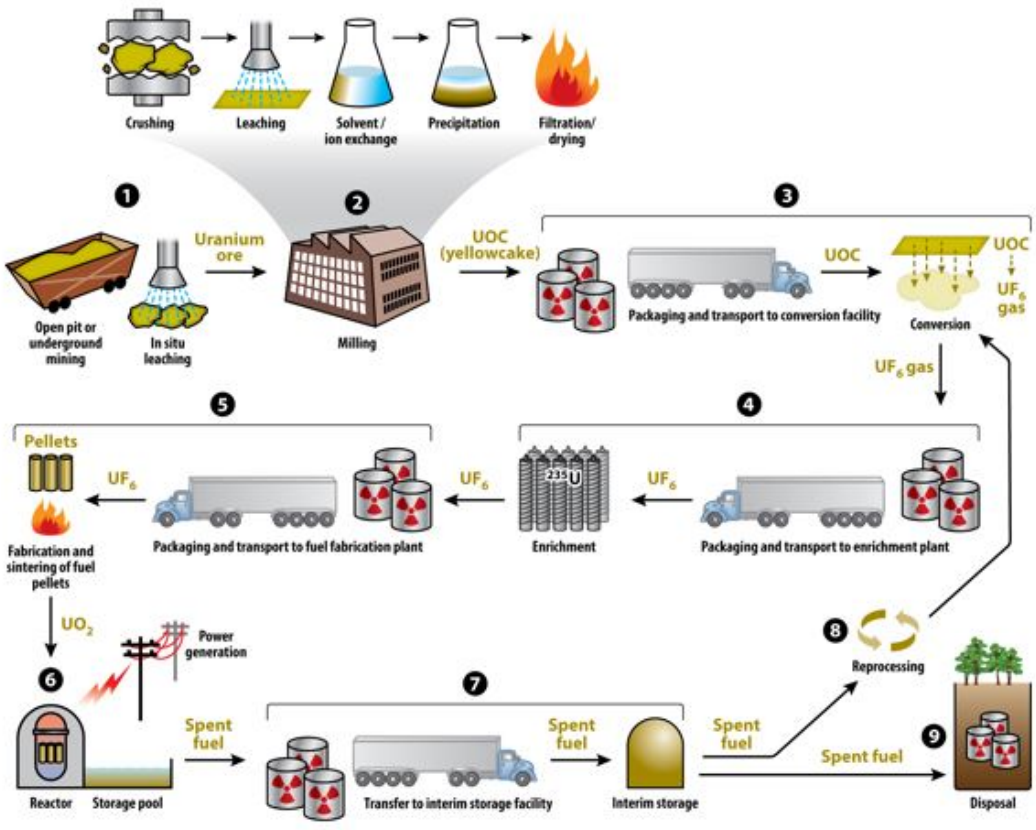

Figure 2.4: Flow chart representation of the nuclear fuel cycle (taken from Ref. [Kri16])

2.3.1 Uranium mining

Uranium mining is carried out in one of three ways depending on the type and location of the ore: open-pit mining; underground mining; and in-situ mining [Kee16]. Until 50 years ago, uranium mining was predominantly open pit mines since the ore was located very close to the surface. With the large demand for uranium, uranium deposits near the surface were soon exhausted and underground mining had to be employed for deposits that were too deep for open cast [Pro11]. The mined uranium ore is crushed and chemically treated (adding acid alkali) to extract the uranium. The remaining crushed rock, termed 'tailings', is then disposed of appropriately [Age09]. In cases where uranium deposit is present in an aquifer in permeable rock, confined in non-permeable rock, in − situ leaching is used. Leaching solution (sulphuric acid or ammonium carbonate) is pumped through the drill holes, into underground deposits, and the liquid, now bearing uranium is pumped out [Šve08]. This method is economical and produces less amount of waste when compared with open cast and underground mining.

2.3.2 Uranium Milling Process

Normally, uranium ore contains a limited amount of uranium-bearing minerals, therefore obtaining uranium from its ore involves several transformation steps. In the initial steps, the solution from the rock is treated to precipitate uranium compounds, dried and calcined to form yellow cake, a yellow solid composed of almost 70% uranium oxide by weight [Age18]. The conversion of uranium ore into yellow cake can be divided into three stages: the first is crushing, the second is grinding, and the third leaching. Crushing involves a process whereby the ore rocks are sprayed with water and a big crusher breaks down the lumps to 200 mm in diameter in particle size. Grinding: the particles are crushed again to 25 mm particle size then mixed with water to prevent dust formation [Sil13]. The fine slurry produced is then leached in sulfuric acid for acidic ore or an aqueous solution containing sodium bicarbonate and sodium carbonate for alkaline ore.

2.3.2.1 Recovery of Uranium from leached solution

The leached solution contains a mixture of cations and anions. Alkaline leaching produces relatively pure solutions in comparison to those produce from acid leaching [Age18]. Acid leaching generates a solution with large amounts

of impurities and very low uranium, therefore the solution must be concentrated and purified. This is achieved by solvent extraction, ion exchange or ELUEX process, which is a combination of the two. If there are undissolved solids present in the solution, they are removed by filtration, decantation, sedimentation or centrifuges [Nas11].

The final product of the mentioned process is in the form of UO_2SO_4 - a sulphate or ($Na_4[UO_2(CO_3)_3]$) - a complex carbonate. The uranium is then precipitated as uranite, filtered and then dried to produce the uranium concentrate known as "yellow cake", a yellow powder of uranium oxide (U_3O_8) [Ko12]. The yellow cake is often then heated to remove impurities thus increasing the concentration of U_3O_8. Although Yellow cake has a uranium concentration of 80%, for uranium to be used as reactor fuel it needs further treatment. This is due to the fact that uranium fuel required should have a greater purity and constant composition [Age18]. Conversion is thus applied to achieve this.

2.3.3 Uranium Conversion Process

In order to use uranium for fuel, uranium concentrate has to be converted into uranium hexafluoride (UF_6), a form usable in other stages of the nuclear fuel cycle [Age09]. Converting U_3O_8 into UF_6 occurs in two stages. In the first stage, U_3O_8 is converted into uranium tetrafluoride (UF_4); a green salt with a melting point of 960°C [Šve08]. The uranium concentrate is dissolved in an acid to obtain $UO_2(NO_3)_26H_2O$(UNH), purified, and then calcined to produce UO_3 powder. This powder is then hydrofluorinate with hydrofluoric acid, which converts it into U_4 [Age15]. In the second stage UF_4 is converted into UF_6 through the fluorination. These two stages are normally carried out at the same plant but can also be carried out at different plants as in the case of hydrofluorination stage with production of UF_4 [Nas11].

2.3.4 Uranium Enrichment Process

Natural uranium consists of three isotopes: ^{238}U at 99.28%, ^{235}U at 0.711% and ^{234}U at 0.0054% [Moo14]. Of the three isotopes, only ^{235}U is fissile and can be used as nuclear fuel in thermal reactors. Although some reactors such as Canadian Deutrium Pressurized Water Reactor (CANDU PWR) and Magnox use natural uranium, they only represent about 10 percent of the worlds

installed reactors [Age09]. The majority of thermal reactors require enriched uranium as fuel, for these reactors, the ^{235}U concentration must be increased to 2-5% by mass through a process termed Enrichment [Nas11]. Gaseous diffusion and centrifugal enrichment are two of the most popular methods of enrichment. Both methods require UF_6 as feed material because of its three main advantages: it is a gas at low temperature; fluorine has only one isotope; and fluorine has a low atomic weight [Sil13].

2.3.4.1 Gaseous diffusion

The rate of diffusion of ^{235}U through a porous membrane is relatively higher than that of ^{238}U, this is used to achieve separation in gaseous diffusion. However, this is an energy intensive process that requires large plants for the operation to be economically viable since the separation factor is low [Age09]. Figure 2.5 is an illustration of gaseous diffusion enrichment process.

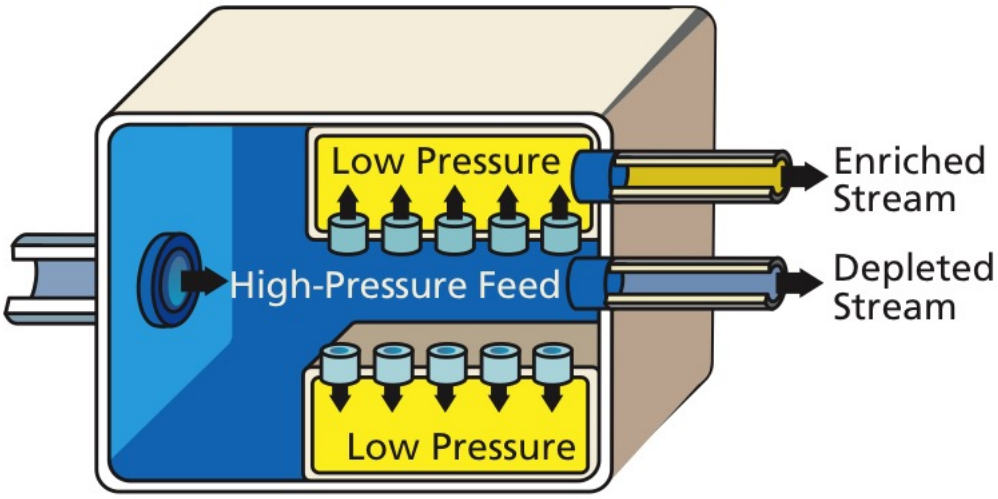

Figure 2.5: Schematic representation of the gaseous diffusion process (taken from Ref. [Com17])

2.3.4.2 Centrifuge enrichment

Uranium is enriched in ^{235}U by introducing UF_6 gas into a centrifuge with rapidly spinning tubes [Ko12]. Centrifuge enrichment relies on the application of extremely high rotational speeds to separate the ^{235}U from the heavier ^{238}U. The weight difference between the two uranium isotopes causes them to

separate into two streams at high speeds; one of enriched uranium (increased ^{235}U concentration) and another of depleted uranium (decreased ^{235}U concentration). ^{235}U then diffuses out of the centrifuge, leaving heavier ^{238}U behind [Sil13]. The enriched UF_6 is then converted into UO_2 which is required for fuel fabrication. Figure 2.6 is a schematic illustration of centrifugal enrichment process.

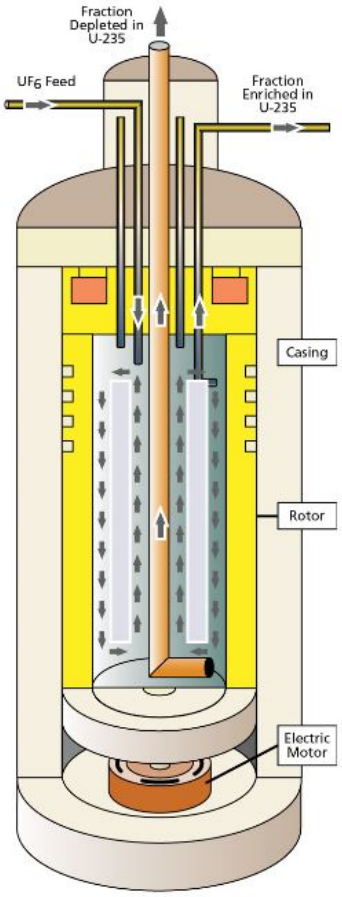

Figure 2.6: Schematic diagram illustrating a basic centrifugal enrichment process (taken from Ref. [Com17]

2.3.5 Fuel fabrication

Following the process of enrichment, the next step is nuclear fuel fabrication. The end product of this stage is nuclear fuel in the form of an assembly of a particular shape and material form suitable for the reactor design. A fuel assembly is made of cylindrical tubes called "fuel rods". These rods contain

uranium oxide pellets contained in zirconium alloy frame [Par11]. Fuel fabrication involves re-conversion of UF_6 to UO_2 powder, pellet fabrication, cladding fabrication, fuel rods fabrication and lastly assembly fabrication. Reconversion is the first step in fuel fabrication process. Several processes, both dry or wet can be used to convert UF_6 to UO_2 powder [Che12]. Figure 2.7 illustrates the steps involved in these processes.

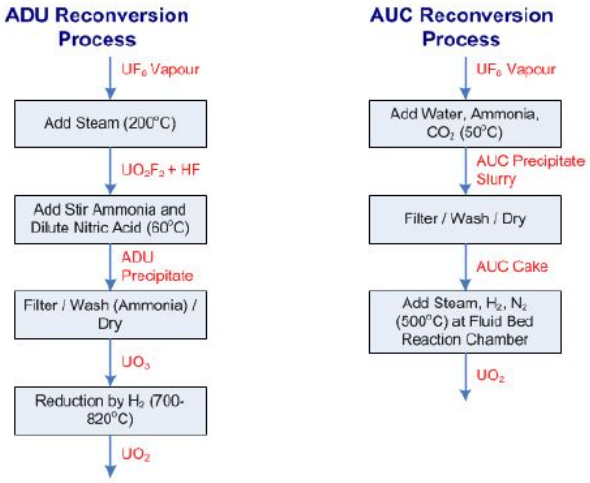

Figure 2.7: Schematic chart of the uranium reconversion process in the nuclear fuel cycle (taken from Ref. [Age09])

Power reactors use UO_2 fuel in the form of ceramic pellets. To fabricate the pellets, ceramic grade UO_2 powder is pressed into a cylinder about the size of a fingertip, baked at high temperature [Šve08]. The pellets are then loaded into long tubes (commonly zirconium alloy or stainless steel) to form fuel elements that make up the reactor core [Sil13].

2.4 Uranium mining in Africa

The development of uranium production in Africa started in the 1920s after the discovery of uranium in the Democratic Republic of Congo (DRC) [Das12, Win17]. The need for clean sources of energy such as nuclear power as an alternative to fossil fuels created a boom in the global demand for uranium. In 2003 power plants consumed double the amount of uranium supplied by the mines [Das12]. To meet the demand, much focus was directed towards Africa.

To date, Africa produces 18% of the worlds annual uranium output. Figure 2.8 shows the areas in Africa that have uranium deposits [Win17].

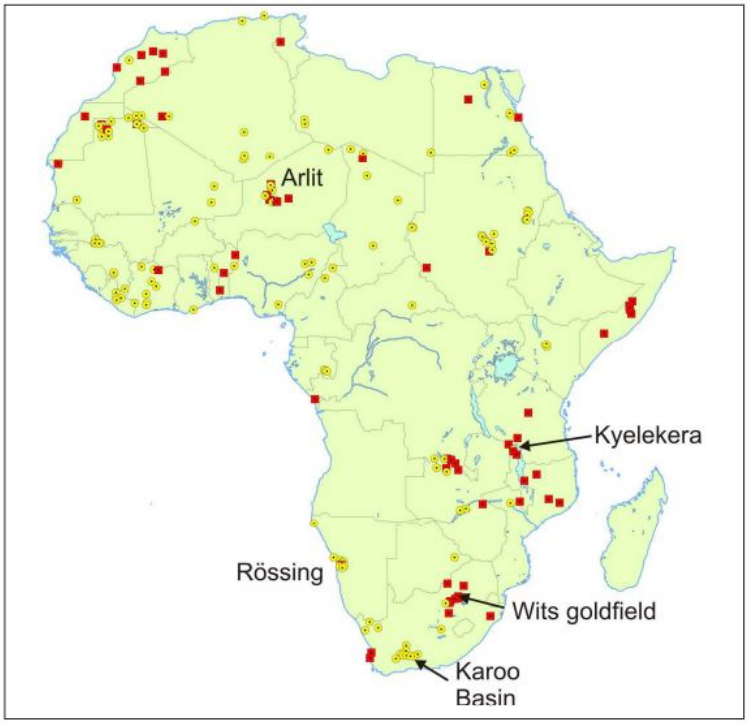

Figure 2.8: Map showing the locations of uranium deposits in Africa. The areas marked with yellow circles show primary deposits, where uranium occurs as the main commodity. The red squares mark secondary deposits, where uranium is a by-product (taken from Ref. [Das12])

Africa has four types of deposits that produce the majority of the uranium. These are [Win17]:

- Archaen quartz conglomerate hosted gold uranium found in South Africa
- Neopreterozoic end-onogeny sheeted leucogranites and small stocks found in Niger and Malawi
- Channel-hosted calcrete found in Malawi and Namibia
- Alluvial deposits found in Namibia

Uranium is a predominant mineral found in Africa. Namibia, South Africa and Niger have been actively mining uranium however it remains untapped in several other African countries [Das12]. Table 2.1 shows some of the African

countries that have uranium prospection and exploration projects.
For the purpose of this study, we will focus on uranium deposits from Botswana and Nigeria. Both countries have untapped uranium resources and are planning to start mining in the near future.

2.4.1 Botswana

The Letlhakane project mentioned in Table 2.1 consists of Gojwane deposits and Serule deposits, with Gorgon, Gorgon South, Kraken and Mokobaesi prospects [Kin16]. In September 2015 the JORC-compliant project total was upgraded to 33,000 tU at 0.0167% U indicated and 108,000 tU inferred resources at 0.0172% U, all at 100 ppm cut-off [Kin16]. The ore is carnotite in calcrete and shallow open-pit mining with acid heap leach is expected to produce 1150 tU per year over a period of 18 years. This will be exported through Namibia. Construction was expected to start in 2018, but has been deferred for two years. In additions to Letlhakane project, Impact Minerals, a company based in Australia was also exploring some prospective deposits in eastern Botswana including Lekobolo. Further south, it had the Shoshong and Ikongwe prospects in calcrete [Kin16]. In 2014 Impact put its uranium exploration on hold [Kin16].

2.4.2 Nigeria

In 2009, Nigeria and Russia signed an agreement allowing for exploration and mining of uranium. Three months after the initial agreement was signed a broader agreement was signed for the construction of a Russian power reactor and a research reactor [Kin16]. Uranium deposits have since been discovered in six states of Cross River, Adamawa, Bauchi, Kano, Plateau and Taraba [Pro19].

Table 2.1: New uranium mining projects in Africa (taken from Ref.[Age18, Pro19])

Country	Project	Status
Botswana	Letlhakane Project	Exploration ongoing
Cameroon	Kitongo deposit	Exploration ongoing
Central African Republic	Bakouma Uranium Project	Exploration ongoing
Chad	Léré, Mayo Kebbi West	
Egypt	Abu Zenima	
	Gabal Gattar	
Gabon	Bagombe	Exploration ongoing
	Mounana	Reclamation ongoing
	Mikouloungou project	Exploration complete
Guinea	Firawa deposit	Exploration ongoing
	Bohoduo prospect	Exploration ongoing
Malawi	Kayelekera mine	Idle
	Kanyika niobium project,	Exploration ongoing
	Livingstonia uranium project	Exploration ongoing
Mali	Faléa uranium/silver project,	
	Samit project	
Mauritania	A238	Exploration ongoing
	Bir En Nar project	Exploration ongoing
	Tiris project	Exploration ongoing
Morocco	Glibat Lafhouda	
	Twihinate prospect	
	Wafagga prospect	
Mozambique	Mavuzi project	Exploration ongoing
Nigeria	Mika	
	Ghumchi	
Senegal	Saraya East deposit	
Somalia	Alio Ghelle deposit, Bur Area	
	Mudug Province deposits	
Tanzania	Kalulu property	Exploration ongoing
	Manyoni project	Exploration ongoing
	Mkuju uranium project	Exploration ongoing
	Mkuju River project	Idle
	Mtonya project	Exploration complete
Western Sahara	Aghracha prospect	
	Matallah prospect	
Zambia	Lumwana copper project	Exploration complete
	Bungua deposits	
	Njame deposit (Chirundu JV)	Exploration ongoing
	Gwabe deposit,	Exploration ongoing
	Mutanga (ex Kariba) project	Exploration ongoing
Zimbabwe	Kanyemba mine project	Exploration complete

2.5 Characteristic parameters of uranium bearing materials

Nuclear forensics is a major piece of the attribution process involving the analysis of nuclear material to find forensic indicators that arise from known relationships between material character and process history [L'An12, Kri16]. Although nuclear forensic science is a fairly new discipline, a large body of work has been and is being conducted on the subject with the focus mainly on methodologies that can be used, applicable measurement techniques, and identification of parameters that can be used to determine the origin of a material.

In recent years, methodologies have been developed and used in forensic investigations to identify the origin of seized nuclear material. The parameters used for such identification are isotopic composition, impurities, geometric dimensions, age and micro-structure [Red09]. Individually, these patterns are not sufficient for source attribution, but collectively, they reduce ambiguities and therefore give a clearer view of the possible origin [Kri16]. Figure 2.9 is a venn diagram showing valid nuclear forensic signatures and how they can work collectively to match a material to an origin.

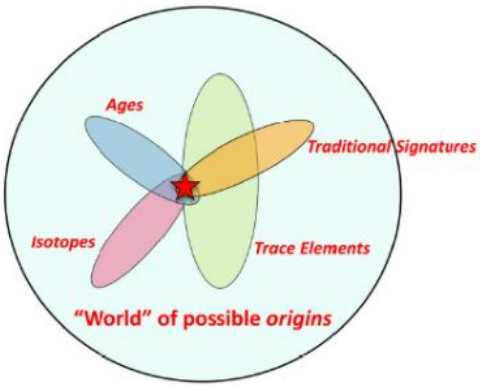

Figure 2.9: Illustration of valid nuclear forensic signatures and the domain of possible material that match those material signatures (taken from Ref. [Gue13])

2.5.1 Isotopic patterns in uranium deposits

Naturally occurring chemical elements show only small variations in the isotopic composition. Once irradiated in a nuclear reactor, these elements undergo nuclear reactions, induced fission (n,f) and neutron capture (n,γ) which alter the isotopic composition of the material to a composition determined by the reactor conditions (neutron energy spectrum, irradiation time, cooling time) [Nic06]. Treatments done in processing such as chemical separation also alter the isotopic composition of chemical elements, thus, creating new patterns that can serve as an identifying fingerprint [Red09]. The information below can be extracted from the isotopic patterns of uranium at different processing stages of the nuclear cycle:

- the different forms in which uranium oxide is found give information on the point of origin in the uranium fuel cycle;
- the detection of small amounts of ^{236}U indicates contamination with recycled uranium and hence points to reprocessing activities;
- the reactor type in which the material was produced can be deduced from the isotopic composition of plutonium.

Natural uranium is described as consisting of isotopes ^{234}U, ^{235}U and ^{238}U. The isotope abundance of ^{235}U has been assumed to be constant at about 0.71 %, however, highly precise inductively coupled plasma mass measurements suggest that the ^{235}U/^{238}U ratio in nature is variable and can be attributed to natural isotope fractionation [Hie12]. Studies have demonstrated that uranium isotope ratios vary in different geologic materials. A number of studies have found isotopic variations in ^{234}U/^{238}U, ^{235}U/^{238}U and ^{236}U/^{238}U ratios in natural uranium ores from different mines [Kea15, Agg16]. Weyer et al. showed that the terrestrial ^{235}U/^{238}U ratio varies over a range of 1.5% in different geological materials [Kri16]. In 2010, Brennecka et al. also studied the ^{235}U/^{238}U ratio of UOC samples in order to relate the variations observed to the U mineralization of the ore [Bre10].

The presence of ^{236}U abundances in higher amounts than those determined in natural uranium samples is an indication of neutron irradiation and reprocessing of the uranium [Sim13]. Srncik et al. [Srn11]in 2011 investigated the

possibility of using ^{236}U abundances within uranium ores as a global nuclear forensics signature, and found significant variations in the ^{236}U/^{238}U ratio for samples from Australia, Brazil and Canada.

From these observations, it was proposed that uranium isotopic ratios were possible viable forensic signatures in ore samples [Kri16]. Although uranium isotope ratios are significant parameters, there are still ambiguities. The same signatures were investigated in UOC but this time there was overlap in some ratios [Kea15]. It is therefore necessary to have several other signatures to reduce ambiguities.

2.5.2 Uranium chronometry

One of the most frequently used methods in nuclear forensic investigations is chronometry. Age is an extremely useful parameter for tracing origin and history. A properly designed chronometric scheme simultaneously provides information on samples composition, enrichment history and time elapsed since last purification [Red09]. Thus serving as an exclusion parameter when searching for the production or processing site. Radioactive isotopes decay at a rate that is determined by the initial amount and half life of the isotope, therefore the ratio of decay product (daughter) to the parent isotope can be used to determine the age of the sample. This can be described using Eqn. 2.14, Eqn. 2.15 and Eqn. 2.16 relating to radioactive decay below [Lil13]:

$$N = N_0 \times e^{-\lambda t} \tag{2.16}$$

$$\frac{N_p}{N_d} = \frac{N_{0,p} \times e^{-\lambda_p t}}{N_{0,p} - N_{0,p} \times e^{-\lambda_d t}} \tag{2.17}$$

$$t = -\frac{ln(1 - \frac{R}{K})}{B} \tag{2.18}$$

where R is measured daughter parent atom ratio
K is decay constant ratio $\frac{\lambda_p}{(\lambda_d - \lambda_p)}$;
B, a factor combining the parent $(\lambda_d - \lambda_p)$ t is the age,
λ_p and λ_d are the parent and daughter decay constants and
N_p and N_d are the amount of parent and daughter nuclides respectively.

2.5.3 Isotopic composition of Stable isotopes

Origin assessment of unknown nuclear material can also be achieved by analyzing the isotopic composition of specific elements [Red09]. Two chemically identical substances have different stable isotope composition if they have different origins or their history is different. lead, strontium , sulphur, neodymium and oxygen are some of the elements that have been successfully validated as signatures for source attribution [Agg16].

- Lead Isotopes

  There are four stable isotopes of Lead: ^{204}Pb, ^{206}Pb, ^{207}Pb, ^{208}Pb. Three of which originate from the decay series of uranium and thorium [Šve08]. Two ratios: n(^{207}Pb/n(^{206}Pb) and n(^{208}Pb)/n(^{206}Pb) have shown significant variations between different uranium mines and geological setting [Rea16]. This was attributed to the age of the deposit and the concentration of the associated parent Uranium and Thorium [Kee16]. In previous studies, Svedkauskait-Le Gore [Šve08] demonstrated that samples from the same geographic location have similar Pb isotopics [Rea16].

  There is a lot of literature on lead isotopes and this is mostly because of its natural variations which could be useful in many geological, environmental and biological investigations [Šve08]. As mentioned before, out of the four stable lead isotopes, only one is primordial, the rest, ^{206}Pb, ^{207}Pb, ^{208}Pb are end-products of radioactive decay of ^{238}U and ^{235}U and the isotope ^{232}Th respectively. The stable isotope composition therefore gives information in the initial U/Th ratio in the mine as-well as the age of the ore. Lead isotopes are chosen because of two advantages: first, production of different lead isotopes from ^{235}U and ^{238}U and also from thorium enables a wider scope for illustration of geological processes; second, Lead isotopes are stable and thus unchanged in the geological environment.

  Lead isotope abundance ratio from different production sites does not vary extensively, therefore, cannot on its own distinguish the origin of a material. It needs to be supplemented with impurity data to resolve any ambiguity issues within a batch of samples being analyzed [Šve08] .

- Strontium Isotopes

  Studied have also been conducted to validate isotopic composition of strontium as a nuclear forensic signature. The variations are due to the age of the deposit and the abundance of alkali metal-rich minerals which vary depending on the geological deposit type [Rea16]. Varga et al. investigated the application of lead and strontium isotope ratio for origin assessment of uranium ore concentrates. Variations were found in the different mine samples and they concluded that lead and strontium isotope ratios were reliable tools for the origin assessment of uranium ore concentrate [Var09]. Mayer et al. also conducted a similar sudy. The isotopic ratio used in the study was $^{87}Sr/^{86}Sr$. The isotopics were found to have variations between 0.70785 - 0.76063, however, there were cases of overlapping between strontium isotopics from different mines. Even though the between mines variation is small, the $^{87}Sr/^{86}Sr$ ratio is less variable in samples of the same origin and less affected by processing. Like lead, strontium isotopics showed natural variations in UOC from different geological origins, although at a lower extent [May13]

- Sulphur and Neodymium isotopes

  Because of the variability of $^{34}S/^{32}S$ in nature, a studies have been conducted to investigate whether this was a valid signature. The $^{34}S/^{32}S$ values in the UOC samples demonstrated significant differences between the samples. $^{143}Nd/^{144}Nd$ also investigated and showed variations dependent on the geological deposit type and the age of the deposit [Rea16, Kra14]. However, the intra-mine variations were lower than those observed for Pb and Sr, and there was overlapping of ratios for some mines, therefore, independently, $^{143}Nd/^{144}Nd$ is not a reliable signature [Kra14].

- Oxygen Isotopes

  For UOC samples, oxygen isotopic may serve as viable signature in nuclear forensic science. In one of his studies, Pajo et al. worked on the applicability of certain parameters: selected impurities and $^{18}O/^{16}O$ ratios, for geo-location in nuclear forensic science. Small changes in $^{18}O/^{16}O$ isotope amount ratios of less than 3% were observed in uranium oxide samples from different mines [May13, Agg16].

2.5.4 Impurities and trace elements

2.5.4.1 Chemical Impurities

During the production of uranium, elements that differ from the wanted radionuclide are present [Kri16]. These elements are called "impurity" elements. Impurities originate from the raw materials used, some are contaminants introduced during the nuclear cycle and others are deliberately added to enhance the performance of the material (support material) [Red09, Agg16]. The impurity spectrum of a material can be a useful parameter for characterization, both comparative and predictive analysis [Peń16].

Determination of other non-radioactive impurities elements can be used to identify nuclear forensic signatures of the process of material production or inherited from the ore body

2.5.4.2 Anionic impurities

The hypothesis that anionic impurities can be used to indicate the chemical process a material has undergone has been the subject of many studies [May13]. Leaching, concentration and purification of different ores are done using chemicals [Peń16].
Baduat et al. developed a methodology to determine the concentrations of anions in uranium ore concentrate samples [May13]. In his study, he looked at variations within the same mine using different sampling methods and again variations within different mines [May13]. It was observed that although there were some differences observed when using different sampling techniques, they were very small as compared to those observed between samples from different mines, thus showing that anion concentration patterns are valid nuclear forensic signature [May13, Kri16]

2.5.4.3 Metallic impurities

Impurities are introduced both intentionally; to improve the final product and for processing nuclear material; or unintentional as contaminates from feed or processing [May13, Red09]. The composition of nuclear material therefore provides important information on the characterization of the material. Analytical techniques such as X-Ray Diffraction (XRD), X-Ray Fluorescence (XRF), Scanning Electron Microscopy with dispersion X-ray spectroscopy (SEM/EDX), thermal analysis or Fourier-Transform Infrared Spectrometry (FTIR) have been proven capable of identifying elemental composition of individual par-

ticles in homogeneous samples such as uranium oxide [May13].

Svedkauskaite-Le Gore et.al [Šve08] pioneered the systematic study on elemental fingerprints for attribution process. In the study, ICP-MS was used in conjunction with statistical analysis methods such as ANOVA, Principle Components Analysis (PCA) and Cluster Analysis (CA) to identify the origin of UF_6 samples. He then concluded that trace impurity analysis was a useful means of characterization and that the impurity fingerprint; although not always unique, was distinctive enough to distinguish between mines [Kri16]. Keegan et al. [Kee16] conducted a similar study, using XRF, ICP-MS and PCA for analysis, he measured trace elemental composition of UOC and found it to be a unique parameter to distinguish three uranium mines in Australia. The impurity pattern was found to be useful in linking UOC samples to their deposit types and geo-source when dealing with larger sample sets [May13].

2.5.4.4 Rare Earth Element (REE) signature

REE are a set of seventeen element, specifically scandium, yttrium and fifteen lanthanides [Zhu17]. Certain impurities are found to have more discriminating power than others, REE (La - Lu) fall among this group [Spa17]. These elements exhibit consistent pattern under different geochemical conditions, therefore, can be used as a forensic signature [Khu18]. REE retain their chemical properties throughout the nuclear cycle. This means that a nuclear material from a single mine, will have the same REE fingerprint as the ore regardless of which stage in the nuclear cycle it was produced.

Many researches have been conducted to investigate the applicability of REE as a nuclear fingerprint. Varga et. al proved that REE patterns are not only indicative of the origin of UOC, but are unaltered by processing, thus, patterns found in UOC correspond to those found in uranium ore [Var17, Red09]. Khumalo et. al and Morton-Bermea et. al also conducted a study on the application of REE for characterization and in both studies it was concluded that REE are good signatures of the original deposit [Khu18].

From these observations REE as well a those from similar studies, it can be concluded that REE can serve as a viable signatures in understanding the formation of uranium deposit and can be used as evidence of uranium origin

[Spa17].

2.5.5 Minerology

Determining the mineralogy of environmental samples for forensic purposes has been done in geo-forensic investigations and potential applications have been identified in Environmental Forensics [Pir11]. However, its is not part of nuclear forensics methodology.

Rock/soil samples are mostly composed of minerals which are derived from the parent material [Daw10]. Therefore, different kinds of minerals have distinctive elemental compositions as well as a great variety of distinctive physical and chemical properties determined by their different structures.

There are several different minerals but in most soils the main minerals which occur at concentrations above 1% consist of approximately 30 common types; quartz, iron oxides, feldspars, sulfates, amphiboles, pyroxenes, aluminium oxides, carbonates, zeolites and clay minerals [Daw10]. The mineralogy can therefore work as a discriminative signature since it is characteristic of the sampling region.

The present work is an investigation into the applicability of some of these signatures: isotopic patterns of U and Th, REE patterns, impurity spectrum and mineralogy of mine ore samples from uranium mining areas in Nigeria and Botswana.

Chapter 3

Methodology

The nuclear forensics field has become a topic of interest in scientific, public policy and popular press literature for almost fifteen years [L'An12]. The "analysis" makes up the core of the forensic investigation and includes, but not limited to radiometric measurement techniques. This chapter describes the analytical techniques applied in nuclear forensics with an emphasis on ICP-MS and XRF as they are applied in the study.

3.1 Sequencing of techniques

Analytical tools used in nuclear forensics are mostly destructive techniques (consume the sample during preparation and analysis) [L'An12]. Therefore, a proper selection and sequencing of techniques should be detailed in the nuclear forensic plan. These techniques are shown in Table 3.1. The sequence followed is based on the data required from the investigation, taking into account the quantity of the sample, information available, and the signature being investigated. [Age15]. A description of nuclear forensics methodology is as follows:

- Uranium isotopic composition
- Uranium concentration
- chemical composition
- sample morphology
- Impurity identification and concentration
- Age
- Characterization of non-nuclear material associated with the sample

Table 3.1: Analytical techniques that can be used to find information on Uranium-bearing materials (taken from Refs. [Red09])

Analytical technique	**Parameter**	**Information**
Optical microscopy	Appearance	Material type
Titration, HKED, IDMS	U, Pu content	Chemical composition
HRGC, TIMS, ICP-MS, SIMS	Isotopic composition	Enrichment (intended use, reactor type)
ICP-MS, GDMS	Impurities	Production process; geo-location
AS, TIMS, ICP-MS	Age	Production date
TIMS, SIMS	$^{18}O/^{16}O$	Geolocation
Profilometry	Surface roughness	Production plant
SEM, TEM	Micro-structure	Production process

HKED, hybrid K-edge dinsitometry; IDMS, isotope dilution mass spectroscopy; HRGS, high-resolution gamma spectroscopy;TIMS, thermal ionization mass spectroscopy; ICP-MS, inductively coupled mass spectroscopy; SIMS, secondary ion mass spectroscopy; GDMS, glow discharge mass spectroscopy; AS. alpha spectroscopy; SEMS scanning electron microscopy; TEMS, transmission electron microscopy

3.2 Applied Measurement techniques

A variety of counting techniques may be used in nuclear forensic analysis of radioactive materials as listed in Table 3.1. Radiometric techniques such as alpha, beta and gamma spectrometry have proven to be great analytical tools. Another valuable technique is mass spectroscopy. This technique is used to determine both elemental and isotopic composition of nuclear materials [Kri11]. In the past, a sequence of techniques was needed in order to determine the spectrum of impurities. Mass spectroscopy techniques such as ICP-MS offers great accuracy, precision and capability to determine not just the radioactive isotopes but also the stable isotopes [L'An12]. X-ray fluorescence (XRF) spectrometry is a well-established, analytical technique in the determination of major elemental compositions of environmental materials. XRF uses X-rays to successfully analyse solid samples non-destructively. Its high accuracy and precision make this technique a favourite method of choice in mineralogy and investigation of the chemical composition of environmental samples, respectively.

The analytical techniques used during the experimental work include mass

spectroscopy using ICP-MS and XRF. This section will introduce the basics of the techniques used in this experimental work.

3.2.1 Inductively Coupled Plasma Mass Spectrometry (ICP-MS)

In the past, several techniques were required to obtain the impurity spectrum of uranium based materials. Although these techniques were sufficient at the time, they lacked sensitivity, were time consuming and the direct determination of impurities was often hampered by matrix and spectral interferences [Šve08]. ICP-MS shown in Fig. 3.1 was thus introduced into nuclear laboratories world wide, allowing reliable measurements of multiple samples. The ICP-MS is a powerful analytical technique commonly used for elemental and isotopic composition of samples by measuring the mass-to-charge ratio of the ionized sample [Swi15]. The technique combines the effective ion generation properties of ICP with the abilities of MS to offer a broad range of capabilities. These include high precision ($< 1\%$ uncertainity), better detection limits (parts per billion (ppb)), higher throughput, the ability to handle both simple and complex matrices, superior detection capability and ability to extract isotopic information [Kri11]. However, there are some drawbacks involved with this technique. It is expensive and requires extensive sample preparation. Another problem is limited number of laboratories with the instrument and scarcity of skilled operators [Kri16]. A description of the mechanism in which ICP-MS analysis occurs follows.

3.2.1.1 Instrumentation

The modern ICP-MS system offers benchtop platforms and is relatively expensive. Major manufactures of this instrument include Thermo scientific, Agilent, perkin Elmer and Bruker [Bor13]. In this study, Agilent instrument was used. Figure 3.1 shows examples of both commercially available Q-ICP-MS systems; Thermo scientific (left) and Agilent 7700 series (right).

Figure 3.1: Inductively Coupled Plasma-Mass Spectroscopy instruments (taken from Ref. [Bor13].)

A typical Q-ICP-MS system consists of six components [Baz12];

- Sample introduction system to turn the sample solution into an aerosol,
- Inductively coupled plasma source to ionize the aerosol,
- A vacuum interface to extract ions from the plasma source and turn them into a positively charged ion beam,
- Ion optics to focus the ion beam,
- Quadrupole mass spectrometer to separate the ions in the beam based on their mass-to-charge ratios,
- Dual mode detector (pulse counting and analogue) to measure the intensity of the separated ions.

Figure 3.2 is a schematic of the Q-ICP-MS system. Each components is discussed in detail below.

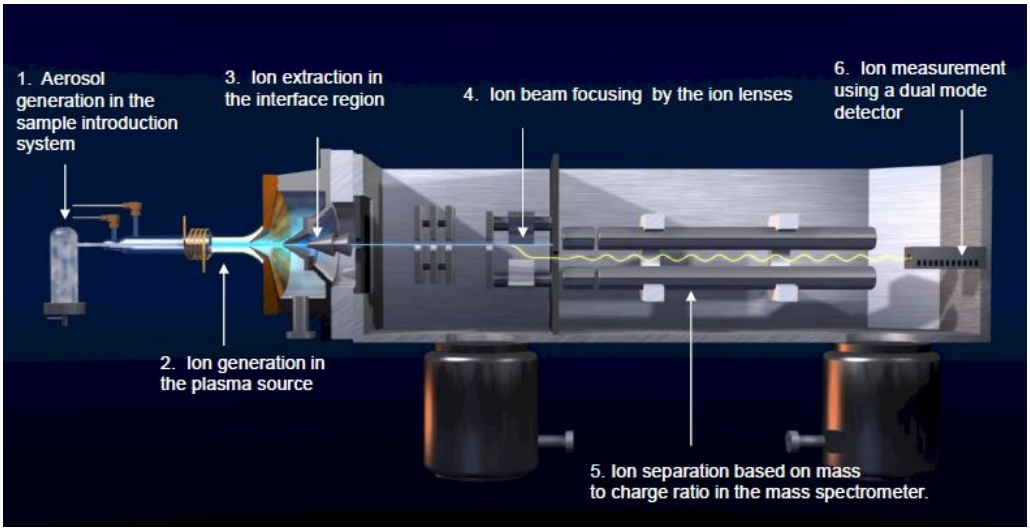

Figure 3.2: A schematic diagram of Quadrupole Inductively Coupled Plasma-Mass Spectroscopy components (taken from Ref. [Bor13])

Introduction system The primary components of the sample introduction system are the nebulizer and spray chamber. A sample is introduced into the system as an aerosol, this is achieved by either aspirating a liquid sample or a dissolved solid sample (as was the case in this study) into a nebulizer or by laser ablation to convert a solid sample directly into an aerosol [Lin09]. The liquid sample is pumped from a vial, via a peristaltic pump, and into the nebulizer [Šve08]. There liquid droplets form on the needle, and are nebulized by argon gas flowing through a second needle that runs perpendicular to the sample needle. The spray chamber then selects very fine droplets (μm) from the aerosol to pass into the plasma [Baz12].

Inductively coupled plasma source The ICP source consists of slightly ionized argon gas at 8000K that is sustained in a quartz torch. The plasma dries, decompresses, atomizes and ionizes the aerosol coming from the spray chamber [Bor13].

Plasma or Vacuum interface At the sampling orifice, ions in the plasma are extracted using a set of cones and an extraction lens. The pressure caused by the vacuum system encourages diffusion of the electrons out of the beam, producing a positively charged ion beam [Bor13].

Ion Optics Electrostatic lenses are used to focus the ion beam and and neutral species are removed[Bor13].

Quadrupole Mass Spectrometer The focused ion beam travels through the quadrupole mass filter where the ions are separated based on their mass-to-charge ratio by rods [Vér10]. An electrostatic filter is established by applying alternating AC and DC voltages to opposite pairs of rods and rapidly switching them along with an RF field. The electrostatic filter only allows ions of a single mass-to-charge ratio pass through the detector rods at a given time. This ability allows the system to produce isotopic information since different isotopes have different mass-to-charge ratios [Bor13].

Duel mode detector After the ions are separated, they must be counted by a detector [Lin09]. The detector translates the number of ions striking the detector into electrical signals that can be measured and related to the number of atoms of the element in the sample using calibration standards [Vér10]. The detectors use a high negative voltage to attract the positively charged ions to the detector. Once the ions hit the active surface electrons are released which then strike the next surface of the detector and amplify the signal [Lin09].

3.2.2 X-Ray Fluorescence

X-ray fluorescence is a well established non-destructive analytical technique that is used to determine the chemical structure of inorganic and organic material as well as chemical composition in liquid and solid samples for elements from Mg to Pu [Hut15]. Different types of samples can be analyzed using XRF; bulk solids such as metals, rocks and ceramic; pressed petals; loose powders; and liquids [Kri11]. XRF has emerged as an efficient and powerful tool for analysis in a wide variety of fields such as, biology, archaeology and forensic science [Sha11].

3.2.2.1 Theory

When X-rays encounter matter, one of the following interactions occur [Hasc14]:

- Absorption and transmission through the sample as in medical X-rays.
- Diffraction and scattering from ordered crystal as in XRD used for crystal structure determination

- Generation of X-rays of different colours as in XRF used to determine elemental composition.

An atom consists of a nucleus (proton and neutron) and electrons. The electron spin in shells (K, L, M, N) at a specific distance from the nucleus and take on discrete (quantized) energy levels. X-ray interaction normally only affect the innermost K and L shells [Mis12]. The highest binding energy is found in the k shell therefore more energy is required to remove an electron from the k shell compared to the L shell.

When a X-ray photon with sufficient energy strikes an atom, an electron is dislodged from the atoms inner shells (k shell). The atom fills the k shell with an electron from the l shell. As the electron drops to the lower energy state, excess energy is emitted as a k_α x-ray. The atom also fills the vacant shell with an electron from the M shell, similarly as the electron drops to the lower energy state, excess energy is released as K_β x-ray.This process produces k-lines. If the x-ray photon does not have sufficient energy to dislodge an electron in the K-shell but enough for the L shell, the electron from the L-shell will be displaced. Electrons from the subsequent M-shell will drop to occupy the vacant L-shell thus releasing L_α and L_β x-rays which form L-lines.

XRF energies for different elements are as follows:

- Organic elements such as H, C, N, O do not give XRF peaks as photons from these elements are so low in energy that they can neither be transmitted through air, nor efficiently detected using silicon based detectors.
- Low Z elements such as Cl, Ar, K, Ca give out only K-lines
- High Z electrons such as Ba, Hg, Pb, U give L-lines. This is because electrons in the K-shell have high binding energy and can not be removed with limited voltage.
- Middle elements Rh-I may give out both K-lines and L-lines.

When inner shell electrons are lost, outer shell electrons drop to lower energy levels to replace them; this process is called fluorescence. During this process atoms produce electromagnetic radiation in the x-ray spectrum (0.01 to 10 nm) [Sha11]. Figure 3.3 illustrates this process. The electron configuration of particular element is defined by the quantum numbers of each electron orbital

[Bor13]. X-rays produced during electron transitions have energies that are characteristic to every element in the sample [Sha11]. XRF spectrometry is an application of this behaviour. The number of characteristic x-rays produced by a sample is directly proportional to the concentration of each element in the sample, thus the chemical composition of a sample can be determined [Vér10].

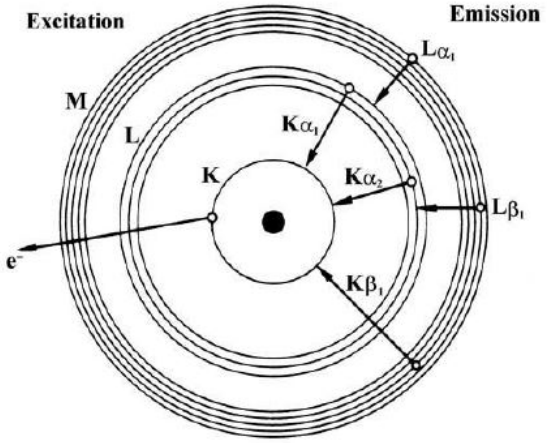

Figure 3.3: A schematic diagram of the Bohr model of an atom. The L-shell electrons are dropping to lower energy levels to replace the lost K-shell electrons, causing a release of photons in the X-ray spectrum. Similarly, M-shell electrons are dropping energy levels to replace the electrons lost by the L-shell. Each transition produces a photon of quantized energy which is measured by XRF (taken from Ref. [Bou14])

XRF spectrometer uses an x-ray tube with Rh, Mo or W anode target to generate a primary x-ray beam that triggers inner shell electron loss in a sample. To replace these electrons, other shell electrons in the sample drop to lower energy levels, causing release of characteristic x-rays [Kri11]. The beam of x-rays replaced is collimated and directed towards a detector (Energy Dispersive XRF) or a crystal (Wave-length Dispersive XRF) [Bor13, Bou14]. Energy Dispersive XRF (ED-XRF) uses multichannel analyzer coupled to a silicon detector to discriminate between different energies of photons in the x-ray beam, each incoming photon is binned by energy and then counted [Wu12]. In Wavelength Dispersive XRF (WD-XRF) however, the characteristic x-ray beam is directed at an angle to a crystal with a given d-spacing [Kri11]. Only the photons with the right energy to solve for Braggs equation at a given angle will remain in phase and be diffracted, directed towards the detector and then

counted. This way any x-ray energy of interest can be selected by changing the angle at which the characteristic x-ray beam reaches the crystal. Numerous crystals with different d-spacing can be used in sequence to measure different elements of interest [Bou14].

Elemental concentrations are quantified relative to a calibration curve for each element. A series of calibration standards are prepared in a similar way to the sample and used to construct a matrix matched calibration curve [Bor13]. There are cases where a calibration curve is impractical, in such cases modern XRF data reduction software can be used to calculate concentration results semi-quantitatively using "fundamental parameters". Assumptions must be made about the geometry, homogeneity and thickness of the sample in order to produce results that are accurate [Bor13]. This method produces results that are within 10% precision.

3.2.2.2 Instrumentation

Most geological and environmental analysis are done using an X-ray tube with Rh target anode [Sha11],The x-ray tube generates characteristic Rh x-rays with enough energy to trigger inner shell electron loss in both light and heavy elements. However, there are certain applications (industrial) where Mo or W anode target is better suited. The voltage and current of the x-ray tube can be altered to optimize the measurement for a specified set of analytes [Bou14]. Primary beam filters can be used in order to remove line overlaps that are caused by characteristic Rh x-rays produced by the x-ray tube [Hasc14]. To minimize interference air molecules with the characteristic x-rays generated, excitation of the sample is generally performed in a vacuum. In the cases were the sample is liquid or a loose powder, helium atmosphere is used instead [Oye18].

3.2.2.3 Analytical issues

Samples that are smaller than the XRF sample holder in size do not require sample preparation [Hasc14]. To obtain the best results, the sample should have a flat and polished face. The samples must be large to completely cover the analytical area of the XRF sample holder. When dealing with smaller samples or measuring small potions of a larger sample, masks of different sizes can be installed to isolate the portion of interest [Bor13].

Modern XRF instruments are capable of analyzing loose powders. The powders are loaded into the instruments sample cups and are held in place by a thin film (normally polypropylene). The film used is transparent to x-rays, therefore the sample is analyzed directly with minimal interference from the film [Gla11].

XRF samples are ideally converted into glass discs or pressed pellets prior to analysis. Although the non-destructive nature of the technique is lost in the process, this sample matrix makes it easier to build a matrix matched calibration [Bou14]. For instances were the sample mass is limited, quantification of the samples composition can be performed under the assumption that, for a particular x-ray tube voltage and current setting, the maximum number of x-rays that a sample can generate theoretically, are produced . For instances where a thin layer of sample is used, especially in the micrometer or nanometre range, the calculations will systematically underestimate the concentrations of heavy elements, generating inaccurate results [Bor13]. To ensure that the results are accurate, when analyzing thin samples, a calibration curve must be built by analyzing a series of calibration standards with the same thickness as the sample [Bor13].

3.2.3 Limitations and merits of XRF over ICP-MS

XRF is a well established and understood technique, applied in several research and industrial settings. It is particularly used where chemical composition data are required while the high precision offered by ICP-MS is unnecessary [Bor13]. Analysis using XRF are non-destructive and rapid, allowing for quick turnover time and relocation of the sample for any additional analysis that is needed [Sta13]. The XRF instrument is also less expensive, more user friendly and more versatile than the ICP-MS and is also used to measure analytes that ionize poorly in ICP-MS [Bor13].

In comparison to ICP-MS, XRF produces results that are less precise and less accurate [Šve08] The measurement detection limits are only of order ppm, which limits the utility of the technique for trace constituent analysis. Elements that are lighter than sodium are difficult to analyze and calibration standards do not exist for many sample matrices. XRF technique also has difficulty resolving interferences in some cases such as U interference in Mo

and Zr [Bor13].

3.3 Experimental procedure

Samples investigated in nuclear forensics encompass different types of matrices. Handling, collection, preservation and storage of these samples are key factors in the quality of the final data produced. Radioactive nuclides and isotopic ratios are the most significant nuclear source of information and are unaltered by chemical perturbations of a system [Red09]. Cross contamination between different samples is however the source of the most uncertainty in the analytes.

In this study, the samples collected were in soil matrix. Soil samples are easily collected, manipulated and stored, and they serve as proficient sorbents of actinides, lanthanides, and transition-metal analytes. Nuclear analytes sorb on soil by wet and dry atmospheric deposition processes, accidental release, and transport activities [L'An12]. The highest concentration of these analytes is near the release points.

3.3.1 Samples chosen for the study

The samples under investigation were collected from mining sites. A total of nine samples were collected: these include four rock samples from four mine areas in west African region of Nigeria and five rock samples from mine areas in southern African regions of Botswana. Both Nigeria and Botswana are planning to start uranium mining processes. Information on the sample origin is summarized in Table 3.2.

Table 3.2: Origin of the samples under investigation

Sample ID	Region	Country
S1	Riruwai	Nigeria
S2	Mika 1	Nigeria
S3	Mika 2	Nigeria
S4	Michika	Nigeria
S5	Serule	Botswana
S6	Serule	Botswana
S7	Serule	Botswana
S8	Serule	Botswana
S9	Serule	Botswana

3.3.1.1 Nigeria

Nigeria is located in west Africa on latitude 4°N to 14°N and longitude 0°E to 16° E occupying a total area 923,768 km^2. Uranium ores found in Nigeria are generally in sedimentary sequence, younger granite complexes and deformed basement rocks with granitoid compositions. Ore types in the region are pyrochlore, monazite, xenotime, uranite, pitchblend, coffinite and antinite. Samples under investigation in this study were collected from Adamawa (Michika), Kano (Riruwai) and Taraba (Mika) regions of Nigeria as seen in Table 3.2. A map of the regions is also shown in Fig. 3.4.

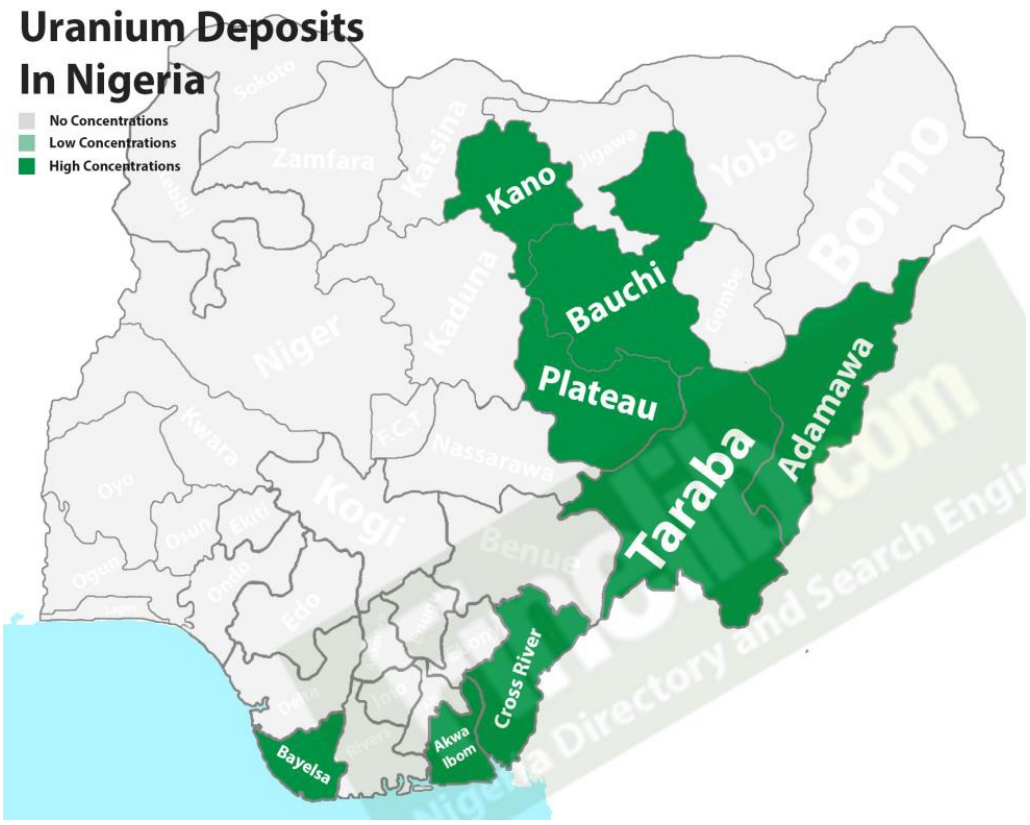

Figure 3.4: Map of Nigeria showing showing sampling regions

3.3.1.2 Botswana

Botswana is located in southern region of Africa. It lies between latitudes 17° and 27°, longitudes 20° and 30° occupying 581,730 km^2 [con19]. Uranium deposits are primarily sandstone hosted roll-front/calcrete deposits, secondary mineralized and primary mineralized , found in Gojwane, Serule and Gorgon

regions. The samples under investigation were sandstone collected from Serule region shown in Fig. 3.5.

Figure 3.5: Map of Botswana showing Serule (yellow dot) where samples were collected (taken from Ref. [con19])

3.3.2 Sample collection

The samples from Nigeria were taken from four different uranium nine regions shown in Fig. 3.2. At these mines, the soil samples were dug using a chisel and mallet and transferred into plastic zip lock bags on site. The bags were labelled as shown in Table 3.2 and transported from Nigeria to University of Witwatersrand (WITS) in Republic of South Africa for subsequent measurement.

The samples from Botswana were taken from one location. Five samples were collected from randomly picked positions across the mining region. At the sampling points, a bucket auger was used to droll into the ground and the samples were collected at a depth of 60 cm. Each sample was transferred into a polythene zip lock bag, weighed and labelled as shown in Fig. 3.2. The

samples were then transported to from Botswana to WITS) for subsequent measurement.

3.3.3 Sample preparation

Sample preparation is a significant part of the analytical process. For better precision and an accurate representation, samples need to be homogeneous prior analyses. To guarantee homogeneity, all the samples collected were taken to the geo-sciences laboratory at WITS for crushing and pulverization. The crushing and milling instruments used are shown in Fig. 3.7 The milling media, grinding discs and beaker were washed with ethanol and in addition extra pure sand was ground before milling of a new sample to dean the mill and avoid cross contamination of between samples. Once milled the samples were then transferred into sealed bags, re-tagged, re-weighted and transferred for storage awaiting analysis. Figure 3.7 shows the different transformational stages (sampling. crushing, milling) the samples went through until they were ready for storage. Preparation and analysis of the samples was conducted at laboratories; WITS analytic laboratory and WITS earth laboratory.

Figure 3.6: Grinding machine and milling machine used in sample preparation

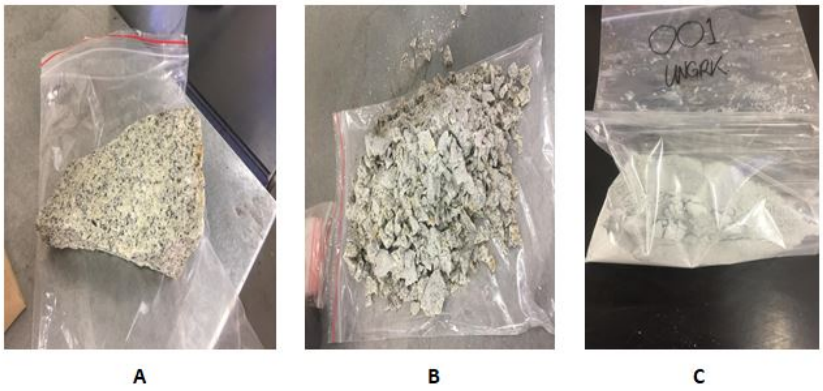

Figure 3.7: Transformational steps in sample preparation

3.4 Experimental technique

The different analysis required in the study were performed using a number of analytical methods. The elemental and isotopic concentrations were determined using ICP-MS and XRF techniques described before.

For XRF the samples were taken to the School of Geosciences Earth LAB where they were analysed using Malvern Panalytical Axios WDXRF spectrometer. Once the experiment was done and measurements were concluded, the results were then provided for further analysis as will be discussed in Chapter 4.

3.4.1 Measurement using ICP-MS

Several techniques can be used for elemental analysis; of these techniques, ICP-MS offers a wider range of detection limits, multi-element analysis,isotopic capabilities and is time efficient. Although highly accurate, ICP-MS can not be directly used on solid samples but requires samples to be in liquid form. Samples in soil matrix, such as those under investigation must therefore be dissolved prior to measurement. In this study, Agilent Technology, 7700 Series ICP-MS was used for analysis.

For complete dissolution of the samples a microwave system shown in Fig. 3.9 was used. Microwave digestion employs high temperature and pressure

to accelerate the process. One of the benefits is that complete dissolution is achieved using nitric acid and hydrochloric acid. Another is that the lower sample to solution ratios lead to better detection limits and the high pressure used prevents some elements from being volatile.

Figure 3.8: Microwave system used for sample preparation

Test samples were taken to determine if the samples contain silica. A mass 0.25 grams of each sample was transferred into teflon microwave vessels in preparation for acid digestion. The samples were diluted with water then mixed with aquarigia (a 1:3 mixture of HNO_3 and HCl respectively) and H_2O_2 then sealed and placed in a microwave. The mixtures were then heated to 200°C in a microwave system shown in Fig. 3.9. The system starts and slowly increases to a maximum of 200°C over a period of fifteen minutes then drops back in ten minutes. Test results showed that there was no silica in any of the samples.

For actual measurement, 0.5 grams of each of the nine samples was taken, duplicated and labelled. The samples were then diluted with 0.5 HCl and nitric acid. Each duplicate was diluted twice, with 10 ml and again with 50 ml making a total of 36 sub-samples for analysis. The digested samples together with the calibration standards (5 ppb, 20 ppb, 50 ppb, 100 ppb, 500 ppb, 1000 ppb), blank samples and quality control samples (20 ppb, 100 ppb) were

introduced to the ICP-MS system to measure the individual elements as well as their isotopes in ppb.

Once the measurements were completed, a report was sent with the concentration estimates of the isotopes. A total of fifty elements were measured in the samples from Nigeria and 40 in the samples from Botswana. The isotopes measured include ^{232}Th, ^{238}U and REE elements which are of particular interest in nuclear forensic studies. The concentrations of the isotopes were provided in units of ppb for the different dilution factors.

3.5 Method of Analysis

A variety of statistical tools are available for analyzing multivarient data. Some of these include Cluster Analysis, Principal Component Analysis and discriminant Function Analysis [Šve08]. For this particular study however, Analysis Of Variance (ANOVA) (significance level $\alpha = 0.5$) was applied to the data. ANOVA is one of the most popular statistical methods for testing a hypothesis [Ali16]. In this investigation it was used to determine which of the elements that form the impurity spectrum of the samples under investigation change significantly with sampling location (origin).

In ANOVA, the total variance of the data set is broken down into two parts; variance within the individual sample group (mining area), and the variance between the different sample groups (mining areas). The variance within a sample group, which is a measure of the variance due to the differences between replicates in an individual sample group is determined using Eqn. 3.1 stated below [Kim17].

$$\sum \frac{(x_i - \bar{x})^2}{n-1}, \tag{3.1}$$

where n is the number of members in a sample group, x_i is a measured value and $\bar{x}$ is the mean of the n measurements. The value obtained using Eqn. 3.1 is termed the Mean of Squares within demoted MS_W. The variance between sample groups which is a measure of the variance due to interaction between sample groups is determined using Eqn. 3.2 [Ali16].

$$\sum \frac{(x_1 - \bar{x_0})^2}{h-1}, \tag{3.2}$$

, where h is the number of groups and $\bar{x_0}$ is the the overall mean of all the measurements. The value obtained from Eqn. 3.2 is termed the Mean of Squares between groups and is denoted by MS_B.

The F-test value is the ratio of Mean of Squares between groups (MS_B) and Mean of Squares within groups (MS_W) shown in Eqn 3.3 [Ali16].

$$F = \frac{MS_B}{MS_W}, \tag{3.3}$$

In order to determine if a variable is statistically significant, the F-critical also has to be determined from the F-Table at $\alpha = 0.05$. This is done by looking at the the value at the point (h-1,n-1). A section of the table of critical values is shown in Fig. 3.10 with the F-critical for this study highlighted in yellow. If the F-test value obtained is larger than the F-critical, then the differences between the samples are not by coincidence and are therefore statistically significant [Kim17]. For a data set with F-test values less than F-critical, no conclusion can be drawn. The p-value is the smallest level of significance at which the hypothesis is rejected. Large p-values indicate a large probability that the differences observed are coincidence [Ali16].

F critical values (continued)

			Degrees of freedom in the numerator								
		p	1	2	3	4	5	6	7	8	9
i in the denominator	8	.100	3.46	3.11	2.92	2.81	2.73	2.67	2.62	2.59	2.56
		.050	5.32	4.46	4.07	3.84	3.69	3.58	3.50	3.44	3.39
		.025	7.57	6.06	5.42	5.05	4.82	4.65	4.53	4.43	4.36
		.010	11.26	8.65	7.59	7.01	6.63	6.37	6.18	6.03	5.91
		.001	25.41	18.49	15.83	14.39	13.48	12.86	12.40	12.05	11.77
	9	.100	3.36	3.01	2.81	2.69	2.61	2.55	2.51	2.47	2.44
		.050	5.12	4.26	3.86	3.63	3.48	3.37	3.29	3.23	3.18
		.025	7.21	5.71	5.08	4.72	4.48	4.32	4.20	4.10	4.03
		.010	10.56	8.02	6.99	6.42	6.06	5.80	5.61	5.47	5.35
		.001	22.86	16.39	13.90	12.56	11.71	11.13	10.70	10.37	10.11
	10	.100	3.29	2.92	2.73	2.61	2.52	2.46	2.41	2.38	2.35
		.050	4.96	4.10	3.71	3.48	3.33	3.22	3.14	3.07	3.02
		.025	6.94	5.46	4.83	4.47	4.24	4.07	3.95	3.85	3.78
		.010	10.04	7.56	6.55	5.99	5.64	5.39	5.20	5.06	4.94
		.001	21.04	14.91	12.55	11.28	10.48	9.93	9.52	9.20	8.96
	11	.100	3.23	2.86	2.66	2.54	2.45	2.39	2.34	2.30	2.27
		.050	4.84	3.98	3.59	3.36	3.20	3.09	3.01	2.95	2.90
		.025	6.72	5.26	4.63	4.28	4.04	3.88	3.76	3.66	3.59
		.010	9.65	7.21	6.22	5.67	5.32	5.07	4.89	4.74	4.63
		.001	19.69	13.81	11.56	10.35	9.58	9.05	8.66	8.35	8.12
	12	.100	3.18	2.81	2.61	2.48	2.39	2.33	2.28	2.24	2.21
		.050	4.75	3.89	3.49	3.26	3.11	3.00	2.91	2.85	2.80
		.025	6.55	5.10	4.47	4.12	3.89	3.73	3.61	3.51	3.44
		.010	9.33	6.93	5.95	5.41	5.06	4.82	4.64	4.50	4.39
		.001	18.64	12.97	10.80	9.63	8.89	8.38	8.00	7.71	7.48

Figure 3.9: A section of F-Table used to determine the F-critical used in ANOVA (taken from Ref. [fta19])

Chapter 4

Data Analysis, Results and Discussion

This study was conducted to find the elemental composition of the uranium mined ore samples and determine the measured characteristics parameters that are relevant to nuclear forensics. In this chapter the experimental results are analyzed and the signatures determined.

Like all other analytical measurements, proper calibration is empirical in obtaining quantitative results. In this work the calibration was performed using a variety of sources to guarantee accuracy for a wider mass range and elemental composition. Calibration standards of known concentrations were prepared for several elements. The actual and measured values were then compared to determine the error in the measurements. Figure 4.1 compares the actual concentration versus the measured concentration of prepared standards for ^{232}Th and ^{238}U. To further reduce the uncertainty in the measurements, duplicate samples were run for two different Dilution Factors (DF) per sample. The measurements were averaged and uncertainty was determined. The prepared blank samples also showed that there was no background interference that could contribute to an error in the measurements.

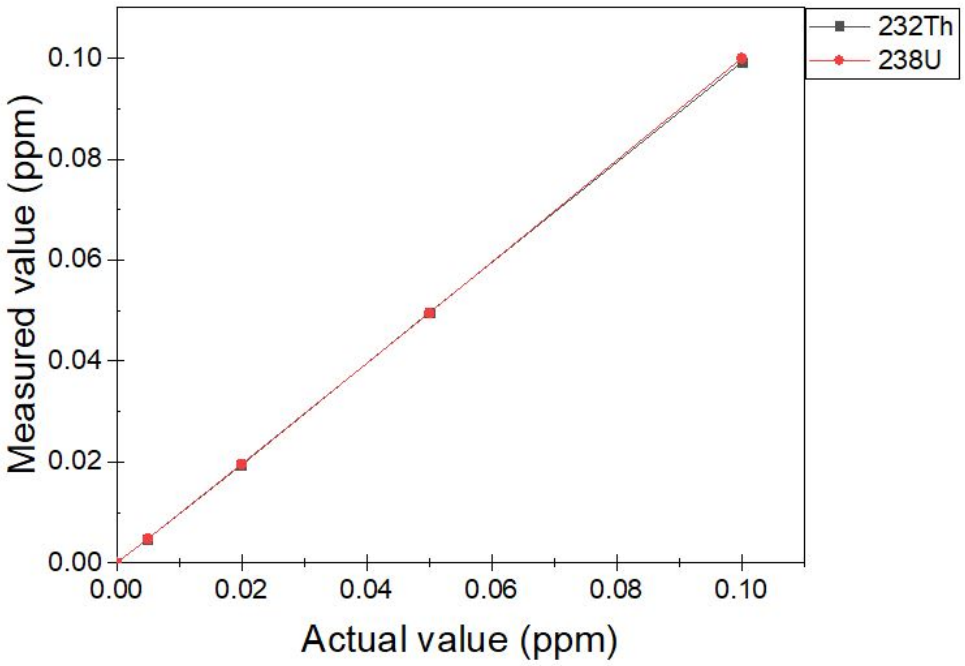

Figure 4.1: Calibration of ICP-MS device with standards for ^{232}Th, ^{238}U radionuclides

4.1 Characterization of uranium mined samples

ICP-MS was used to determine the elemental and isotopic concentrations of sample under investigation. XRF was only applied on the samples from Botswana to determine the major compounds in the samples. The isotopic and activity concentration of ^{232}Th, ^{238}U and ^{238}U are shown in Table 4.1 and Table 4.2. Using these results the activity ratio of the individual samples was determined. Table 4.3 shows the ativity ratios ^{232}Th/^{238}U and ^{235}U/^{238}U determined. These parameters are of particular interest in nuclear forensic investigations.

4.1.1 Uranium and Thorium composition in the samples

The concentrations of ^{235}U was not determined directly from the ICP-MS measurements. However, the isotopic abundance of uranium is constant in nature, (99.27% ^{238}U, 0.711% ^{235}U) [Lil13, Moo14]. Therefore the concentration of

^{235}U can thus be determined from the concentration of ^{238}U by applying Eqn. 4.1.

$$C_{U235} = \frac{0.0711}{99.27} \times C_{U238}, \tag{4.1}$$

where C_{U235} and C_{U238} are the concentrations of ^{235}U and ^{238}U respectively. The results for the uranium and thorium concentrations for the individual regions are summarized in Table 4.1.

Table 4.1: Isotopic concentrations of ^{232}Th, ^{238}U and ^{235}U in the measured samples including their uncertainties.

Sample ID	Isotopic concentration (ppm)		
	^{232}Th	^{238}U	^{235}U
S1	5.410 ± 0.032	1.318 ± 0.050	0.010 ± 0.00
S2	0.055 ± 0.007	0.084 ± 0.003	0.001 ± 0.00
S3	0.159 ± 0.003	73.965 ± 1.371	0.536 ± 0.010
S4	0.061 ± 0.002	7.854 ± 0.293	0.057 ± 0.002
S5	8.812 ± 0.705	2.651 ± 0.212	0.019 ± 0.002
S6	12.208± 0.976	5.304 ± 0.424	0.038 ± 0.003
S7	12.578± 1.006	3.508 ± 0.281	0.025 ± 0.002
S8	8.016 ± 0.641	2.542 ± 0.203	0.018 ± 0.001
S9	6.797 ± 0.544	3.010 ± 0.241	0.022 ± 0.002

Figure. 4.2 show the composition of isotopes ^{232}Th, ^{238}U and ^{238}U in the measured uranium mined ore samples.

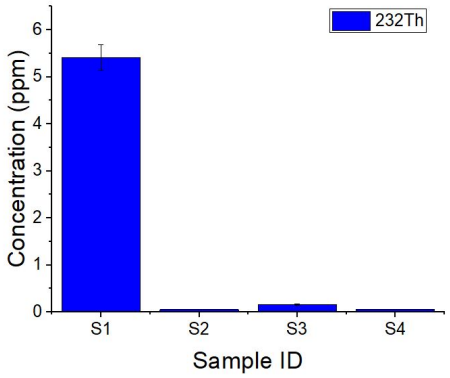

(a) ^{232}Th concentration in S1, S2, S3, S4.

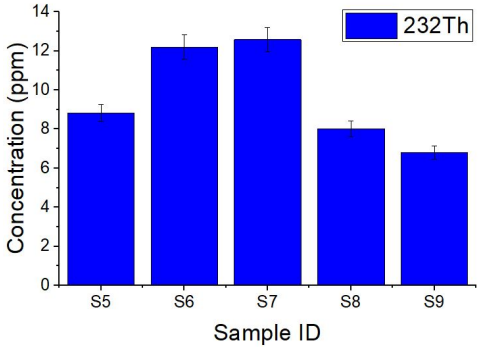

(b) ^{232}Th concentration in S5, S6. S7, S8, S9.

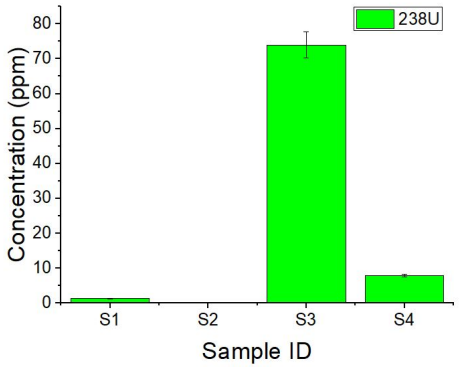

(c) ^{238}U concentration in S1, S2, S3, S4.

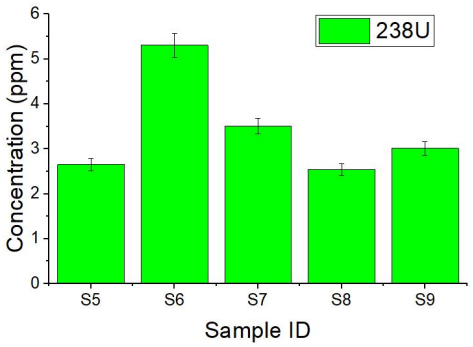

(d) ^{238}U concentration in S5, S6. S7, S8, S9.

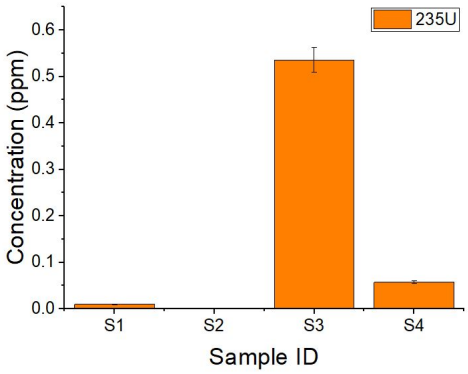

(e) ^{235}U concentration in S1, S2, S3, S4.

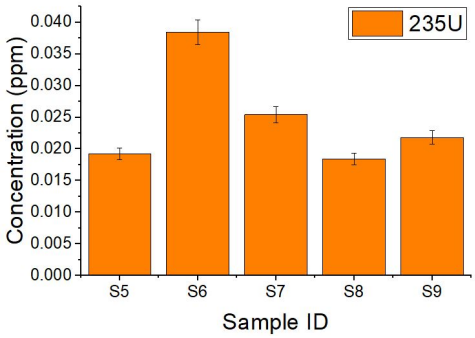

(f) ^{235}U concentration in S5, S6. S7, S8, S9.

Figure 4.2: ^{232}Th, ^{238}U and ^{235}U isotopic concentration in the samples

- ^{232}Th

According to literature, the average crustal elemental concentrations of ^{232}Th is in the range 8-12 ppm [Erd03]. S1, S2, S3, S4 and S9 have ^{232}Th concentrations ranging from 0.055 ± 0.007 to 6.797 ± 0.544 ppm. This range falls below the average crustal concentration. S5, S6, S7

and S8 range from 8.016 ± 0.641 to 12.578± 1.006 ppm and fall within the average range. Given that S1 - S4 are from Nigeria and S5 -S9 are from Botswana, we can conclude that generally, Nigeria samples can be identified by ^{232}Th concentrations that are less than the world average. The samples from Botswana had one out-layer S9 which had concentration less than the continental average but overall, Botswana samples are within the world average.

The samples from Nigeria (S1 - S4) shown in Fig. 4.2a with the exception of S2 and S4 showed significant differences in the values measured for ^{232}Th concentration. S2 had an average concentration of 0.055±0.007 ppm and S4 of 0.061±0.002 ppm. There was an overlap in the concentrations between the two regions, therefore the concentration cannot be used to distinguish between regions.

From 4.2b the samples from Botswana (S5 - S9) had slightly different values; S5 and S8 had values 8.812±0.705 ppm and 8.016±0.641 ppm respectively which are not significantly different. S6 and S7 had values 12.208±0.976 ppm and 12.578±1.006 ppm which are also not significantly different. Therefore for these regions, isotopic concentration of ^{232}Th was not distinct enough to pin point the origin but can be used to narrow down the possibilities locally.

There was a significant difference when comparing the two countries. The concentrations obtained for Nigeria ranged from 0.055±0.007 ppm to 5.410±0.318 ppm while those from Botswana ranged from 6.797±0.544 ppm to 12.578±1.006 ppm. Given that the values do not overlap, ^{232}Th isotopic concentration could be used to distinguish between the countries.

- ^{238}U and ^{235}U

The average crustal elemental concentrations of ^{238}U ranges from 2-3 ppm [Erd03]. S1 and S2 had concentrations of 1.318 ± 0.050 ppm and 0.084 ± 0.003 ppm which are less than the world average. S5, S7, S8, S9 had concentrations ranging from 2.542 ± 0.203 to 3.010 ± 0.241 ppm which fall within the world average range. The remaining samples, S3, S4, S6 had concentrations ranging from 5.304 ± 0.424 to 73.965 ± 1.371

ppm which are greater than the world average . S4 had a significantly higher concentration of 73.965±1.371 ppm in comparison with all the other regions. Overall, the samples from Botswana can be characterized by ^{238}U concentrations that are within the world average range. The samples from Nigeria have concentrations that vary vastly.

From Fig. 4.2c and 4.2e, ^{238}U and ^{235}U followed the same trend. For both isotopes, S3 had the highest concentrations. S1, S2, and S4 had relatively lower concentrations ranging from 0.001±0.00 to 0.057±0.002 ppm and unlike with ^{232}Th concentration,there were no concentration overlaps. The ^{238}U and ^{235}U concentrations are therefore unique signatures in the regions under study

S5, S6, S7, S8, S9 bars in the Fig. 4.2d, there were slight differences in the isotopic concentrations of ^{238}U and ^{235}U. This showed that the isotopic concentrations obtained were characteristic of that area and did not vary significantly at different points within the region. The characteristic isotopic concentration of ^{238}U and ^{235}U was found as taken as 2.403±1.009 ppm, and 0.024±0.007 ppm respectively.

The concentrations from Nigeria range from 0.084±0.003 ppm to 73.965±1.371 ppm which was much broader than the range found in Botswana samples of 2.542±0.203 ppm to 7.854±0.293 ppm. In addition, by comparing the difference between Botswana and Nigeria concentrations, it was also be concluded that ^{238}U concentration could also be used to distinguish between samples from the two countries.

4.1.2 Activity concentration of uranium samples

The natural radioactivity of an environment is due to its geological and geographical conditions. These conditions are related to the activity concentrations of Th, U and K of each rock type and have different levels in soil across the different regions of the globe [Baj15]. For the purpose of this study, the focus is primarily on Th and U. The elemental concentration of these two radionuclides can be converted into activity concentration in terms of Bq.kg^{-1} using Eqn. 4.2 that follows [Baj15]:

$$A_E = \frac{\lambda_E N_A f_{AE}}{M_E C}, \tag{4.2}$$

where A_E is the activity concentration of the nuclide E in the sample, M_E, λ_E and f_E are the atomic masses (kg.mol^{-1}), decay constant (s^{-1}) and the measured elemental concentrations (ppm) of E respectively. N_A is Avogadros number (6.023$\times$ 10^{23} atoms.mol^{-1}) and C is a constant with the value 10^6.

The activity concentrations of ^{232}Th and ^{238}U can also be calculated from their measured elemental concentrations using the IAEA recommended conversion factors stated below [Baj15, Erd03];

$$1.0ppm(^{232}Th) = 4.06 \times A(^{232}Th), \tag{4.3}$$

$$1.0ppm(^{238}U) = 12.4 \times A(^{238}U), \tag{4.4}$$

$$1.0ppm(^{235}U) = 80 \times A(^{235}U), \tag{4.5}$$

where A(^{232}Th), A(^{238}U), A(^{235}U) are the activity concentrations of ^{232}Th, ^{238}U and ^{235}U in units of Bq.kg^{-1}. Determining the activity concentrations for Th and U using Eqn. 4.2 is consistent with the conversion factors shown in Egn. 4.3, 4.4 and 4.5 given by the IAEA. The activity concentration serves as a valuable parameter in nuclear forensics. Table 4.2 shows the specific activity concentrations of ^{232}Th, ^{238}U and ^{235}U for the samples.

Table 4.2: Activity concentrations of ^{232}Th, ^{238}U and ^{235}U in the measured samples including their uncertainties

Sampling region	[Activity] (Bq.kg^{-1})		
	^{232}Th	^{238}U	^{235}U
S1	22.013 ± 1.292	16.410 ±0.621	0.765 ± 0.029
S2	0.225 ± 0.027	1.048 ±0.032	0.049 ± 0.020
S3	0.648 ± 0.010	920.670±17.059	42.913 ± 0.795
S4	0.246 ± 0.008	97.767 ±3.645	4.557 ± 0.170
S5	35.95±1.798	32.87±1.644	1.54±0.077
S6	49.81±2.490	65.77±2.288	3.08±0.154
S7	51.32±2.566	43.50±2.175	2.04±0.102
S8	32.71±1.635	31.52±1.576	1.47±0.737
S9	27.73±1.389	37.32±1.866	1.75±0.087

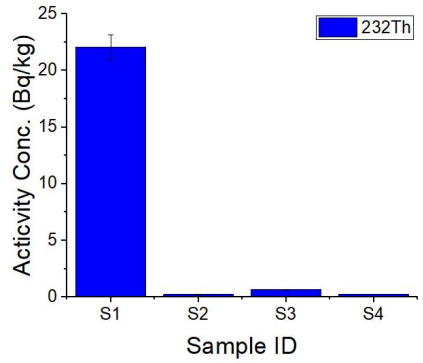

(a) ^{232}Th concentration in S1, S2, S3, S4.

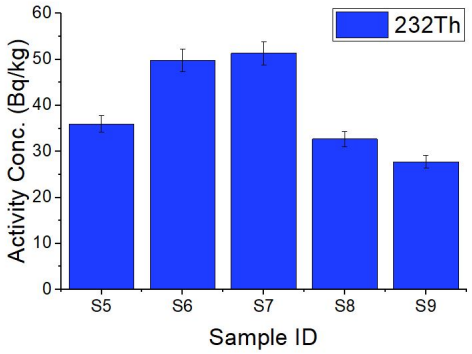

(b) ^{232}Th activity concentration in S5, S6. S7, S8, S9.

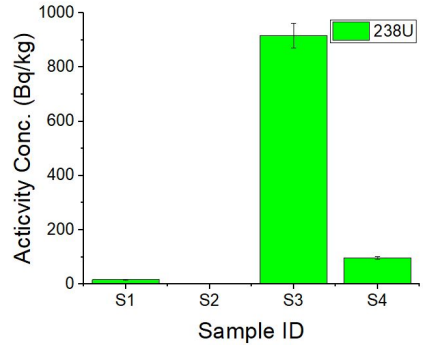

(c) ^{238}U activity concentration in S1, S2, S3, S4.

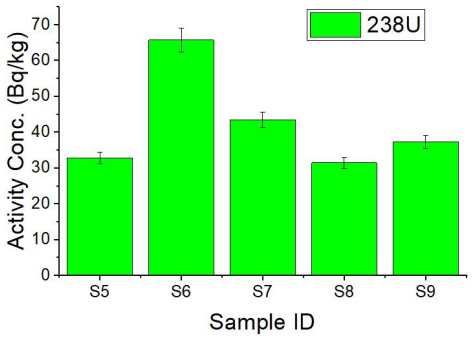

(d) ^{238}U activity concentration in S5, S6. S7, S8, S9.

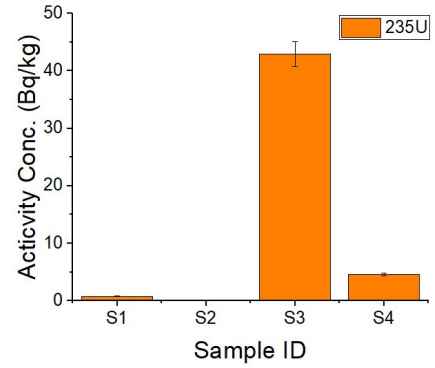

(e) ^{235}U activity concentration in S1, S2, S3, S4.

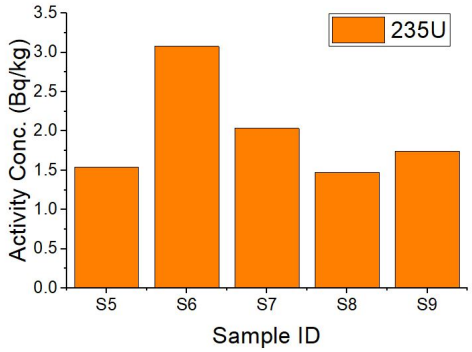

(f) ^{235}U activity concentration in S5, S6. S7, S8, S9.

Figure 4.3: ^{232}Th, ^{238}U and ^{235}U activity concentration in the samples

- ^{232}Th

The average activity concentrations of ^{232}Th in the continental crust and in soil are 44 Bqkg^{-1} and 37 Bqkg^{-1} [Max13]. S1, S2, S3 and S4 from Nigeria and S5, S8 and S9 from Botswana, all had activity concentrations ranging 0.225 $\pm$ 0.027 to 32.71$\pm$1.635 ppm lower than the continental

averages. S6 and S7 had activity concentrations of 49.81±2.490 Bqkg^{-1} and 51.32±2.566 Bqkg^{-1} with significantly higher values than the continental averages. Samples from Nigeria are therefore characterized by activity concentration that are extremely lower than the continental averages, whereas, samples from Botswana yielded both varying and higher concentrations, respectively.

From Fig 4.3a, S1 had the highest activity concentration. S2, S3, S4 had relatively lower concentrations ranging from 0.225±0.027 Bqkg^{-1} to 0.650±0.010 Bqkg^{-1}. Since there were small differences in the values, particularly from S2 and S4, the ^{232}Th activity concentration of these regions were not unique signatures.

The activity concentration of S5, S6, S7, S8, and S9 shown in Fig. 4.3b had slight variations and fell within a small range. The concentrations ranged from 27.73±1.387 Bqkg^{-1} for S9 to 51.32±2.566 Bqkg^{-1} for S7. The activity concentration obtained were therefore characteristic of the region.

All the samples from Botswana had higher activity concentrations in comparison to samples from Nigeria thus activity concentration of ^{232}Th can be used to distinguish between counties.

- ^{238}U and ^{235}U

From literature, average activity concentrations of ^{238}U in the continental crust and soil are 36 Bqkg^{-1} and 22 Bqkg^{-1}, respectively [Max13]. S1 and S2 had concentrations of 16.410 ±0.621 ppm and 1.048 ±0.032 ppm that were significantly less than the continental averages. S3 and S4 had values 917.169±16.994 Bqkg^{-1} and 97.395±3.631 Bqkg^{-1} which were much higher than the continental averages. The samples from Botswana had concentrations ranging from 37.32±1.866 to 65.77±2.288 Bqkg^{-1} higher than the continental crust with the exception of S5 and S8 which were found to have activity concentration of 32.87±1.644 Bqkg^{-1} and 31.52±1.576 Bqkg^{-1}. In both cases, the results show larger uranium activity concentration in the soil.

S1, S2, S4 had distinct values as shown in Fig 4.3 that vary from 1.044±0.032 to 97.936±16.994 Bqkg^{-1} and 0.049±0.002 to 4.557±0.170 Bqkg^{-1}. Therefore in these regions, the ^{238}U and ^{235}U activity concentration were found to be unique signatures.

The activity concentration shown in Fig. 4.3d and 4.3f of S5, S6, S7, S8, and S9 had small variations. This showed that the activity concentrations obtained were characteristic of that region and did not vary significantly at different points within the same region.

4.1.3 Activity ratio of Uranium samples

Table 4.3: Activity concentration ratios ^{232}Th/^{238}U and ^{235}U/^{238}U in the measured samples

Sample ID	^{232}Th/^{238}U	^{235}U/^{238}U
S1	1.35	0.047
S2	0.215	0.047
S3	0.001	0.047
S4	0.002	0.047
S5	1.094	0.047
S6	0.757	0.047
S7	1.179	0.047
S8	1.037	0.047
S9	0.743	0.047

The activity ratio of ^{232}Th/^{238}U, shown in column 2 of Table 4.3 for S2, S3, S4, and S9 were distinctly lower than the continental average of 1.2 [Max13]. Only S1 had a value that was higher than the continental average. S5, S7 and S8 had values that were slightly lower than the continental average. Also there were significant differences in the values obtained for most of the samples except for S3 and S4 which had values 0.001 and 0.002, respectively. The ^{232}Th/^{238}U activity ratio for all the samples ranged from 0.001 to 1.179. In contrast, the activity ratio for ^{235}U/^{238}U, was equal to the continental average of 0.047 for all the samples, this was evident because the natural abundance of ^{235}U was used to determine its isotopic concentration from the measured isotopic concentration of ^{238}U. From these results, ^{235}U/^{238}U activity ratio was not quite unique and did not differ according to sampling region, but ^{232}Th/^{238}U activity

ratio could be identified as a unique signature applicable in nuclear forensic investigations in Nigeria and Botswana.

The results of the characterization of the regions can therefore be summarised as follows:

- In the Riruwai region, the isotopic concentrations of ^{232}Th, ^{238}U and ^{238}U were 5.410±0.318 ppm, 1.318±0.050 and 0.010±0.000 ppm, respectively. The activity concentration of ^{232}Th, ^{238}U and ^{238}U were found to be 22.075±1.296 Bqkg^{-1}, 16.348±0.619 Bqkg^{-1} and 0.765±0.029 Bqkg^{-1}, respectively. And the activity ratio ^{232}Th/^{238}U was 1.35.

- In Mika 1 the isotopic concentrations of ^{232}Th, ^{238}U and ^{238}U were 0.055±0.007 ppm, 0.084±0.003 ppm and 0.001±0.000 ppm. The activity concentration were 0.225±0.027 Bqkg^{-1}, 1.044±0.032 Bqkg^{-1} and 0.049±0.002 Bqkg^{-1} respectively. The activity ratio ^{232}Th/^{238}U was 0.215.

- In Mika 2, the isotopic concentrations of ^{232}Th, ^{238}U and ^{238}U were 0.159±0.003 ppm, 73.965±1.371 ppm and 0.061±0.002 ppm. The activity concentrations were 0.650±0.010 Bqkg^{-1}, 917.169±16.994 Bqkg^{-1} and 42.913±0.795 Bqkg^{-1}, repectively. The activity ratio ^{232}Th/^{238}U was found to be 0.001

- In Michika, the isotopic concentration of ^{232}Th, ^{238}U and ^{238}U were 0.061±0.002 ppm, 7.854±0.293 ppm and 0.057±0.002 ppm, respectively.The activity concentrations were found to be 0.247±0.008 Bqkg^{-1}, 97.395±3.631 Bqkg^{-1}, 4.557±0.170 Bqkg^{-1}, respectively. And the activity ratio ^{232}Th/^{238}U was 0.002.

- In Serule, the isotopic concentration of ^{232}Th, ^{238}U and ^{238}U were 9.682±2.207 ppm , 2.403±1.009 ppm, and 0.024±0.007 ppm, respectively. The activity concentrations of 232Th, 238U and 238U were found to be 39.50±9.415 Bqkg^{-1}, 42.42±12.506 Bqkg^{-1} , and 1.97±0.585 Bqkg^{-1}, respectively. The activity ratio was 0.962 with a standard deviation of 0.179.

4.1.4 Rare Earth Elements

Samples from uranium mines were analyzed to determine the REE concentrations. According to literature [Spa17], the REE concentrations vary with origin. The aim of this research is to investigate signatures that can be added to a nuclear forensic library. To achieve this, samples from different mines need to be compared. Normalizing the REE data using chondrine values is one way to achieve this. The REE data in this study were normalized to examine the statistical variations. Figures 4.4 to Fig. 4.6 illustrate these variations in S1 to S9.

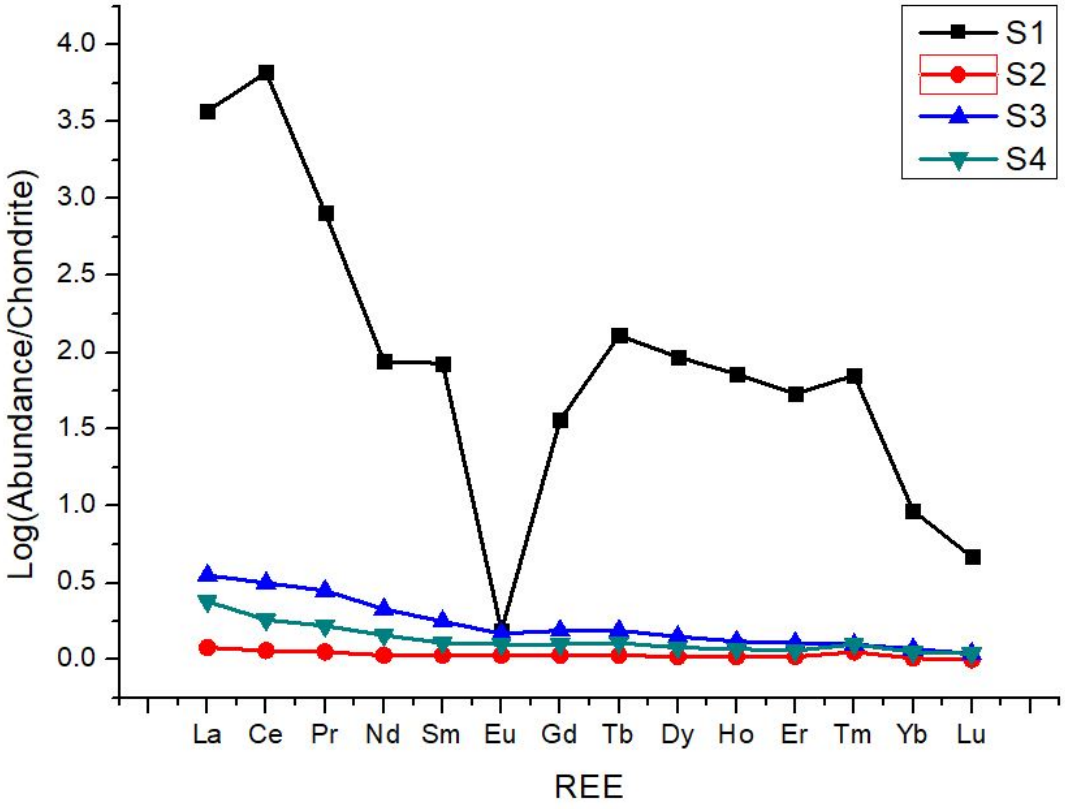

Figure 4.4: REE concentration for S1,S2, S3 and S4 obtained from ICP-MS analysis of results

From Fig. 4.4, it was evident that the S1 had the highest concentrations of all the elements while the lowest concentrations were found in S2. The normalized REE pattern is indicative of a close relation to the between all the samples. The line spectrum for S1, S2, S3 ans S4 follow the same distinctive trends.

The REE bar graphs in Fig. 4.5 were similar for all the Nigeria samples under investigation. S1, S2, S3 and S4 had peaks at Cerium (Ce), Lanthanum (La) and Neodymium (Nd), although at varying concentrations. To determine the significance of these variations, ANOVA was also applied on the dataset. The results of the analysis are discussed later in Section 4.3.

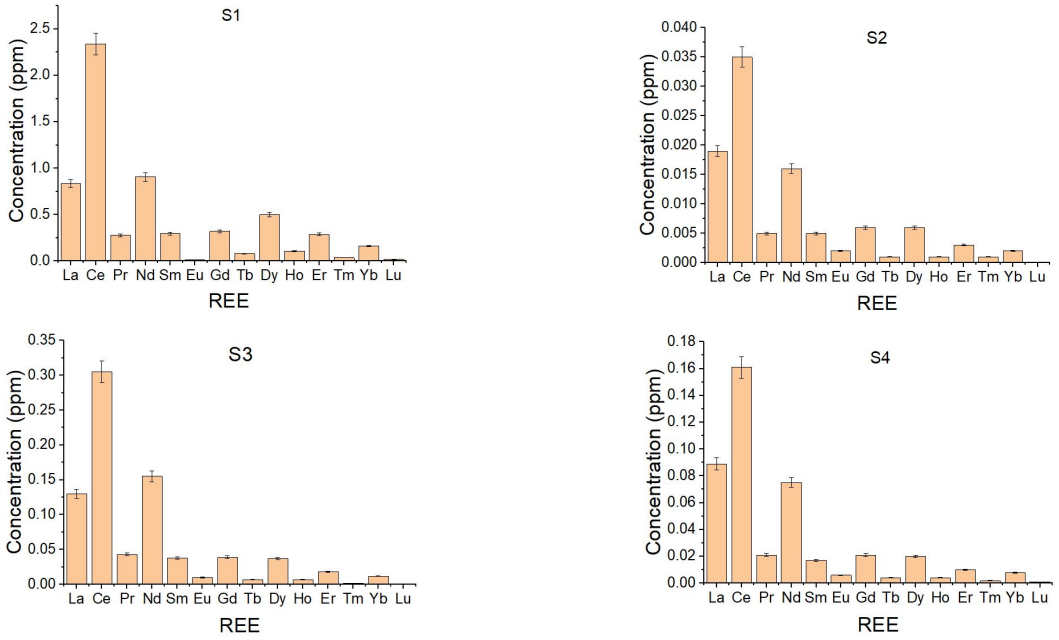

Figure 4.5: Bar charts of REE concentrations for S1, S2, S3, S4 as observed from ICP-MS measurements

The REE pattern shown in Fig. 4.6 indicates a match between all the samples. Also, Fig. 4.7 showed that the elemental concentration of REE at all the sampling points fell within a small range for samples S5, S6, S7, S8 and S9. The shapes of the normalized plot as well as the bar graphs formed were all similar and formed peaks at the same elements (La, Ce, Nd). The values obtained for the elemental concentrations were therefore characteristic of the region.

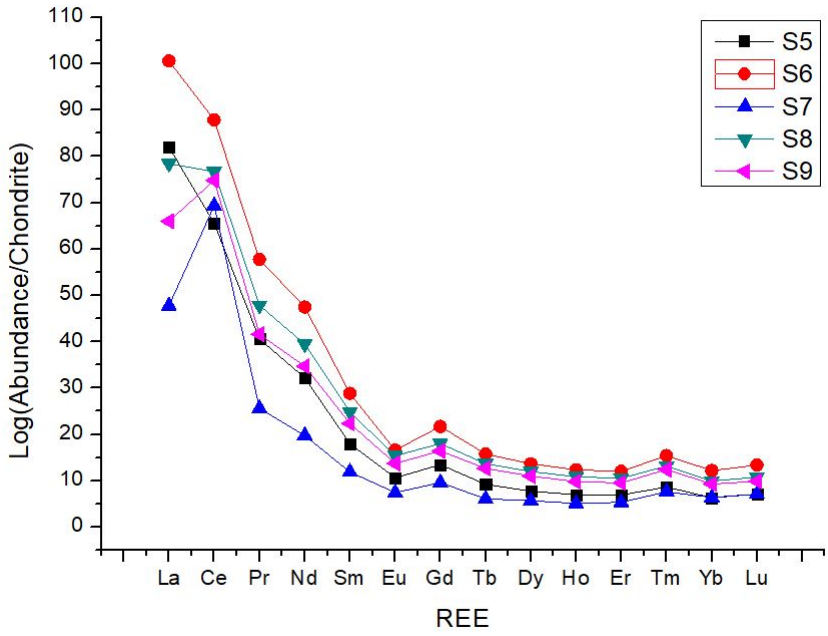

Figure 4.6: REE concentration for S5, S6, S7, S8 and S9 obtained from ICP-MS analysis of results

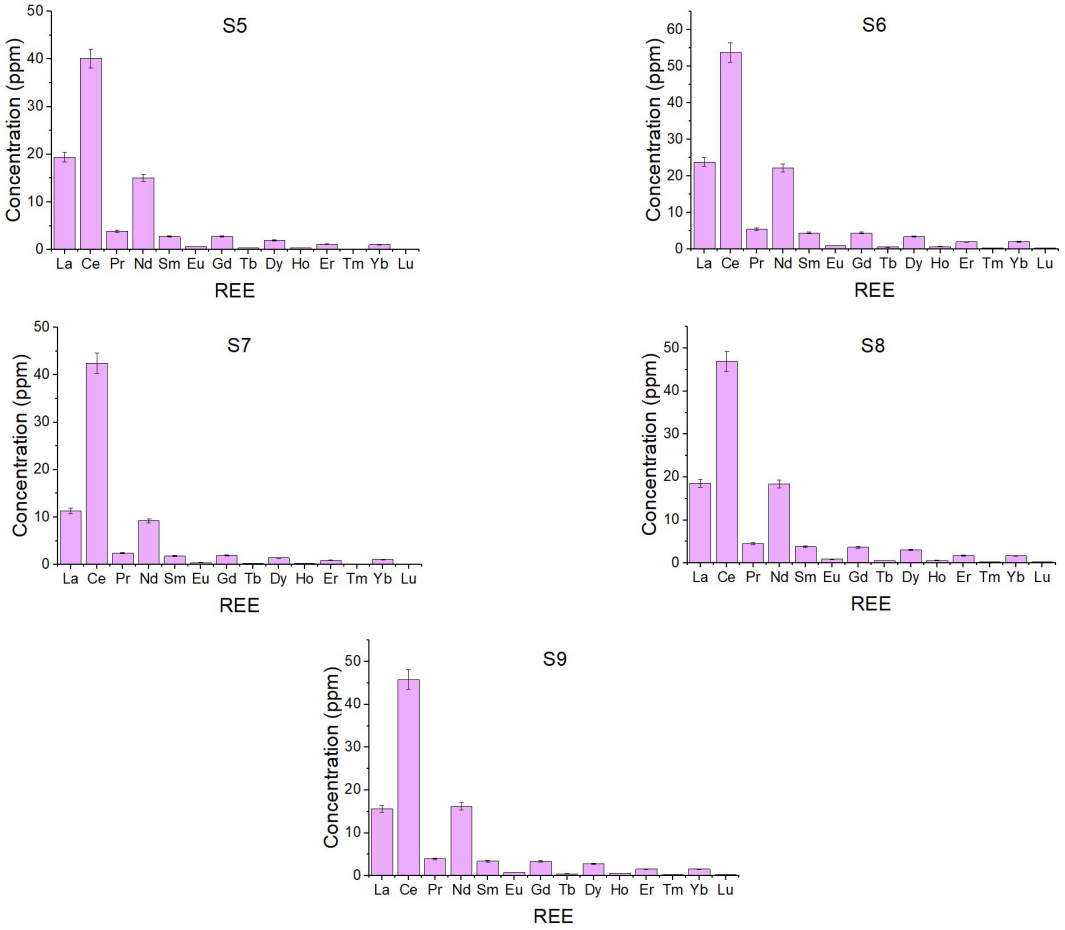

Figure 4.7: Bar charts of REE concentrations for S5, S6, S7, S8, and S9 as observed from ICP-MS measurements

Fig. 4.8 shows the differences in normalized REE pattens for the regions. From the graph S1, S2, S3, S4 indicate a very close match. The same is observed with S5, S6, S7, S8 and S9. There is however a great difference between the two groups. This indicates that S1 - S4 are from one regions and S5 - S9 from another. The REE spectrum is therefore a viable signature for source attribution.

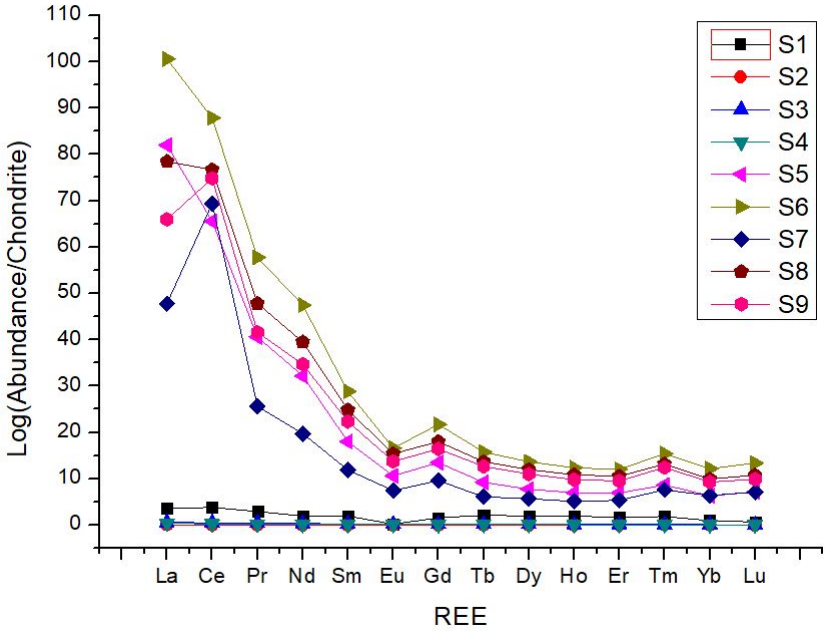

Figure 4.8: Normalized REE for all samples obtained from ICP-MS analysis of results

4.1.5 Impurity Elements

Turning to Figures 4.9 and 4.10 the concentration of the individual elements that form the impurity spectrum varies according to the sampling region. The overall shapes of the spectrums formed for each region were different. S1 had its major peaks at Mg, Ba, Rb and Pb. S2 had major peaks at Ba, Pb, Zr and Sr, while S3 had major peaks at Ba, Pb, Zr, Ba. S4 had peaks at Mg, Cr, Zn and Ba. Therefore the differences displayed by impurity elements were not only different in the concentrations of these elements but the shapes of the spectrum formed were also significantly different. To determine if these differences had any significance, the impurity data were subjected to ANOVA. These results are shown in Section 4.3 that follows.

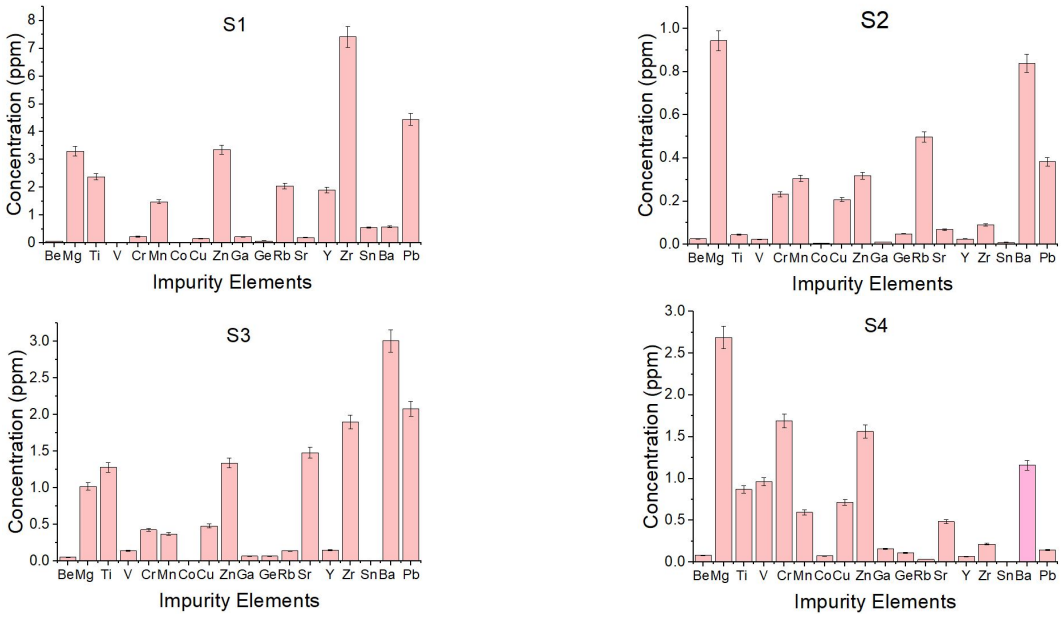

Figure 4.9: Bar charts of impurity elements concentration for S1, S2, S3, S4 as observed from ICP-MS measurements

Samples S5 - S9 shown in Fig. 4.10 followed the same trend. Although at varying concentrations; the impurity elements displayed peaks at Zr, Ba, P, respectively. Zr had the highest abundance in S5, S6 and S7. For S8 and S9, Ba had the highest abundance. Therefore, the elemental concentration of impurities was not characteristic of this region but varies at different points.

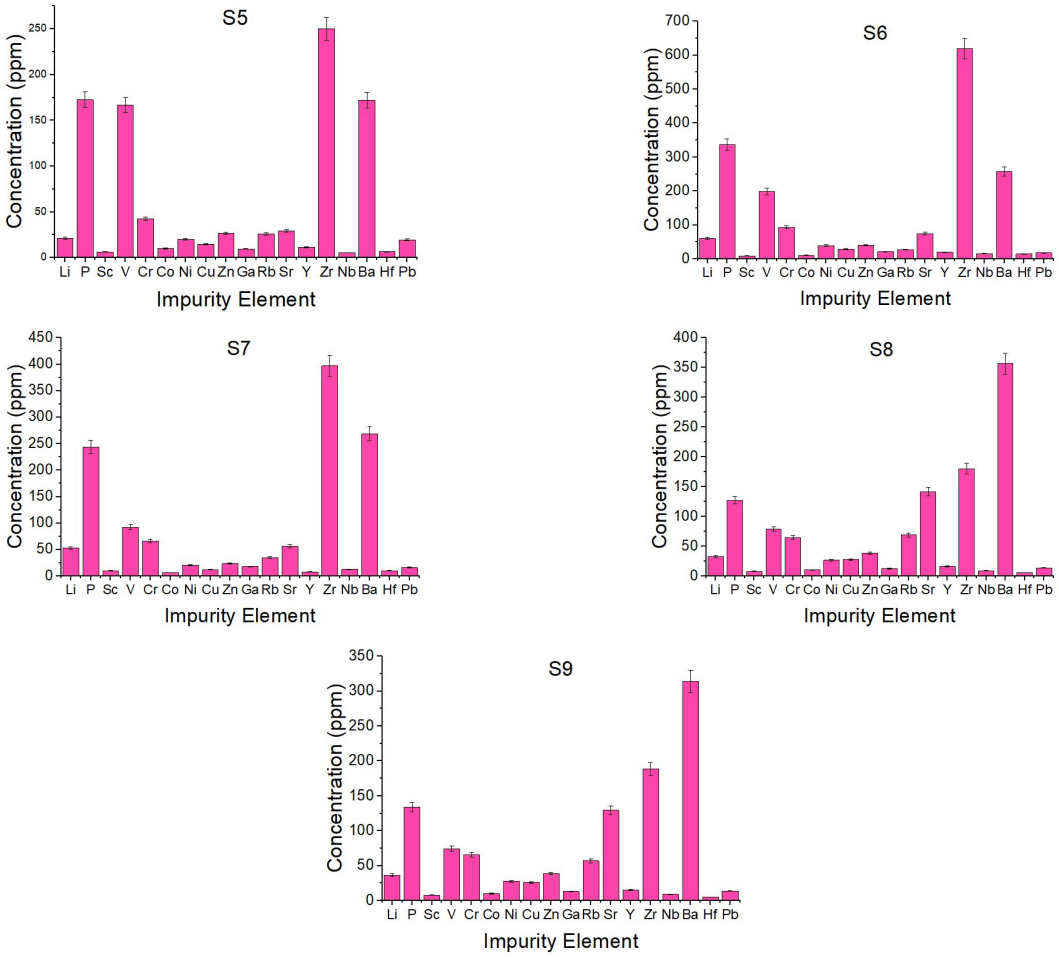

Figure 4.10: Bar charts of impurity elements concentration for S5, S6, S7, S8 and S9 as observed from ICP-MS measurements

4.2 Statistical Analysis of result

The difference in the means of two mutually independent groups can be determined by comparing them using student T-test. However, when determining the differences in means of three or more groups, the most popular method is the one way ANOVA. The ANOVA test is also referred to as F-test. ANOVA was applied to the REE data and impurity data in order to determine if there was any statistical significance in the differences displayed in the results of the samples under investigation. The F-value, significance P-value and F-critical for the samples are shown in Table 4.4 and Table 4.5 .

4.2.1 Results of ANOVA analysis on Rare Earth Elements (REE)

Table 4.4: REE F-statistics for S1, S2, S3 and S4 samples

Nuclide	F-value	F-critical	P-value
La	7.016	3.49	0.006
Ce	6.329	3.49	0.008
Pr	6.979	3.49	0.006
Nd	1.123	3.49	0.379
Sm	6.361	3.49	0.007
Eu	21.725	3.49	3.85E-5
Gd	7.739	3.49	0.004
Tb	7.851	3.49	0.003
Dy	7.224	3.49	0.005
Ho	undefined	3.49	underfined
Er	6.841	3.49	0.006
Tm	7.212	3.49	0.005
Tb	7.288	3.49	0.005
Lu	7.228	3.49	0.077

From Table 4.4, the F-values for all nuclide observed were greater than the F-critical . This indicates that the differences in the values measured were not due to chance. Also the P-values obtained were low, which indicates a very low probability that the differences were just a coincidence. Therefore the REE elements were statistically significant in this case and were relevant to nuclear forensic studies of samples from Nigeria. One nuclide, Ho, was undefined and no conclusion was taken regarding its applicability.

4.2.2 Results of ANOVA analysis on Impurity elements

Table 4.5: Impurity element F-statistics for S1, S2, S3, S4 samples.

Nuclide	F-value	F-critical	P-value
Be	6.040	3.49	0.009
Mg	92.955	3.49	1.420E-8
Ti	483.416	3.49	8.926E-13
V	374.786	3.49	4.048E-12
Cr	5.561	3.49	1.779E-10
Mn	304.108	3.49	1.269E-8
Cu	5.561	3.49	1.779E-10
Zn	304.108	3.49	1.269E-8
Ga	302.000	3.49	0.012
Ge	4.444	3.49	1.396E-11
Rb	426.813	3.49	1.455E-11
Sr	216.620	3.49	0.025
Y	789.474	3.49	1.871E-12
Zr	1649.814	3.49	5.865E-16
Mo	1261.581	3.49	2.919E-15
Cs	195.749	3.49	1.187E-10
Ba	44.804	3.49	8.571E-7
W	4.271	3.49	0.029
Hg	84.944	3.49	2.239E-8
Pb	429.043	3.49	1.814E-12

Similar to the REE analysis, the impurity elements F-values were significantly higher than the F-critical value. This proved that there was a significant difference in the impurity element concentrations between the different regions of Nigeria. The impurity spectrum was therefore a relevant signature for Nigerian samples.

Unlike samples S1-S4 from Nigeria, all samples from Botswana (S5-S9) were taken from the same mine(one group). We can therefore only determine the variance within one mine. Given that for proper analysis we need both variance within a group(mine) and variance between a groups(mines) ANOVA could not be applied on the data.

4.3 Mineral identification and quantification

The mineralogy of soil samples from Botswana (Serule) was investigated using XRF measurements for quarts, aluminium oxide and hematite. Table 4.6 shows the major minerals identified in the samples.

Table 4.6: Major minerals in S5, S6, S7, S8 and S9

Sample ID	SiO_2 (wt%)	Al_2O_3 (wt%)	Fe_2O_3 (wt%)
S5	82.89	7.8	3.07
S6	71.91	14.91	2.15
S7	74.65	14.61	1.8
S8	70.77	9.35	3.07
S9	72.46	9.7	9.7

Quartz (SiO_2) was identified as the most dominant mineral ranging from 70.77 wt% for S8 to 82.89 wt% for S5. The abundance of Aluminium oxide (Al_2O_3) ranged from 7.2 wt% for S5 to 14.91 wt% for S6. Hematite (Fe_2O_3) ranged from 1.8 wt% for S7 to 3.07 wt% for S1 and S8. Other minerals MnO, MgO, CaO, Na_2O, K_2O, TiO_2, P_2O_5, Cr_2O_3 were identified and were found to have abundances less than 1 wt%

Chapter 5

Conclusion and Recommendations

The principal aim of this characterization was to identify reference in uranium ores that could be added to a nuclear forensic database. To achieve this, an investigation on the uranium mine ores from nine sites in two countries was conducted. The uranium mine ores were characterized and the potential use of the parameters obtained for nuclear forensic purposes were determined.

During the investigation, it was observed that ^{232}Th, ^{238}U and ^{235}U isotopic concentration and activity concentration of the sites vary extensively and form part of unique fingerprint. The activity ratio ^{232}Th/^{238}U for the uranium mine sites was found to vary within sites, therefore it also forms part of the fingerprint. However, the same cannot be said about the activity ratio ^{235}U/^{238}U. The ratio was the same for all the sites thus excluding it from forming part of a unique fingerprint. The concentration of ^{235}U was not directly measured using ICP-MS but was calculated from the ^{238}U. This therefore produced concentrations that are not precise and no variations could be observed. The REE and impurity data set of samples from Nigeria were subjected to ANOVA. From the results of the analysis, it was found that both the REE and impurity fingerprints are distinct enough to distinguish between the mining sites.
A nuclear fingerprint of the mine samples can therefore be created using the following:

- Isotopic concentration and activity concentration of ^{232}Th, ^{238}U and ^{235}U
- Activity ratio ^{232}Th/^{238}U
- Rare Earth Element concentration

- Impurity element concentration

On the mineralogy of uranium samples from Serule, it was established that even though there were slight variations in the concentrations of the minerals, Quartz was the dominant mineral in all the sites of the region. This data can be added into a library for reference. The minerology of the mines in Nigeria was not determined and therefore a comparison between the composition of the two countries could not be performed.

5.1 Recommendations

Based on the results obtained from ICP-MS measurements of uranium ore samples from different geological locations, future projects should be based on Eastern, Central and Northern African regions in order to provide a near-complete overview of the signatures. Therefore, a nuclear forensic database to include all other African regions where uranium exploration is feasible is recommended for future research highlights.

It was also observed that the nuclear fingerprints obtained did not only vary for the different countries, but they also vary locally and can be used to distinguish between mines within a country. Hence, a study of the viable signatures that can be used to distinguish between mines in the same country is recommended.

Bibliography

[Age09] International Atomic Energy Agency. Nuclear Fuel Cycle Information System. *International Atomic Energy Agency, Vienna*, IAEA-TECDOC-1613, 2009.

[Age15] International Atomic Energy Agency. Nuclear Forensics in Support of Investigations. *Number 2-G (Rev. 1) in Implementing Guides. International Atomic Energy Agency*, Vienna, 2015.

[Age18] International Atomic Energy Agency. *Integrated nuclear fuel cycle information systems*. Accessed on 2018-11-30.

[Agg16] S.K. Aggarwal. Nuclear forensics: what, why and how. *Current Science*, 2016.

[Ali16] Z. Ali and S. Bala Bhaskar. Basic statistical tools in research and data analysis. *Indian journal of anaesthesia*, 60(9):662, 2016.

[Bae11] A. Baeza *et al.,* Analysis of the different source terms of natural radionuclides in a river affected by norm (naturally occurring radioactive materials) activities. *Chemosphere*, 83(7):933-940, 2011.

[Baj15] A.D. Bajoga *et al.,* Radioactive investigation of norm samples from southern kuwait soil using high-resolution gamma-ray spectroscopy. *Radiation Physics and Chemistry*, 116:305-311, 2015.

[Baz12] A. Bazilio and J. Weinrich. The easy guide to: Inductively coupled plasma-mass spectrometry (icp-ms), 2012.

[Bor13] L. Borg and I. Hutcheon. Forensic analysis of samples from the nuclear fuel cycle. 2013.

[Bou14] M. Bounakhla and M. Tahri. X-Ray Fluorescence analytical techniques. *National Center for Energy Sciences and Nuclear Techniques (CNESTEN), Rabat, Morocco*, 2014.

[Bre10] G.A. Brennecka *et al.,* Natural variations in uranium isotope ratios of uranium ore concentrates: Understanding the 238u/235u fractionation mechanism. *Earth and Planetary Science Letters*, 291(1-4):228-233, 2010.

[Bry18] J.C. Bryan. Introduction to nuclear science. *CRC Press*, 2018.

[Com17] U.S. Nuclear Regulatory Commission. Uranium enrichment, 2017. Accessed on 2019-28-05.

[Che12] J. Chen *et al.,* Back-end of nuclear fuel cycle in china. *Progress in Nuclear Energy*, 54(1):46-48, 2012.

[con19] Wikipedia contributors. Serule, 2019. Online accessed on 20 March 2019.

[Cro12] Ian Crossland. Nuclear fuel cycle science and engineering. *Elsevier, 2012.*

[Das12] N. Dasnois. Uranium mining in africa: a continent at the centre of a global nuclear renaissance. 2012.

[Daw10] L.A. Dawson and S. Hillier. Measurement of soil characteristics for forensic applications. *Surface and Interface Analysis: An International Journal devoted to the development and application of techniques for the analysis of surfaces, interfaces and thin films*, 42(5):363-377, 2010.

[Eic18] G.G. Eichholz. Principles of Nuclear Radiation Detection. *CRC Press, 2018.*

[Erd03] G. Erdi-Krausz *et al.,* Guidelines for radioelement mapping using gamma ray spectrometry data: Also as open access e-book. *International Atomic Energy Agency*, 2003.

[Fed15] V. Fedchenko. The New Nuclear Forensics: Analysis of Nuclear Materials for Security Purposes. *Oxford university press*, 2015.

[fta19] Z score table, 2019. Accessed on 2019-05-13.

[Gla11] M.D. Glascock. Comparison and contrast between XRF and NAA: used for characterization of obsidian sources in central mexico. In *X-ray fluorescence spectrometry (XRF) in geoarchaeology*, pages 161-192. Springer, 2011.

[Gue13] R. Guenther *et al.,* India-United States cooperation on global security: Summary of a workshop on technical aspects of civilian nuclear materials security. *National Academies Press*, 2013.

[Has14] F. Hasani *et al.,* Naturally occurring radioactive materials (norms) generated from lignite-fired power plants in kosovo. *Journal of environmental radioactivity*, 138:156–161, 2014.

[Hasc14] M. Haschke. XRF-basics. In *Laboratory Micro-X-Ray Fluorescence Spectroscopy*, pages 1-17. Springer, 2014.

[Hie12] J. Hiess *et al.,* $^{238}U/^{235}U$ systematics in terrestrial uranium-bearing minerals. *Science*, 335(6076):1610-1614, 2012.

[Hut15] I.D. Hutcheon *et al.,* Nonproliferation nuclear forensics. Uranium: Cradle to Grave. *Mineralogical Association of Canada*, pages 377-394, 2015.

[Iaea17] IAEA Incident. trafficking database (itdb). Incidents of nuclear and other radioactive material out of regulatory control: *Fact Sheet*, 2017.

[Joy11] D. Joyner. Interpreting the nuclear non-proliferation treaty. *Oxford University Press, 2011.*

[Kea15] A.C. Keatley *et al.,* An investigation into heterogeneity in a single vein-type uranium ore deposit: Implications for nuclear forensics. *Journal of environmental radioactivity*, 150:75-85, 2015.

[Kee16] E. Keegan *et al.,* Nuclear forensics: Scientific analysis supporting law enforcement and nuclear security investigations, 2016.

[Ken09] W.E. Kennedy, Jr. Naturally occurring radioactive material (NORM V): proceedings of an international symposium, Seville, Spain, 19-22 March 2007. *Radiation Protection Dosimetry*, 138(3):286-289, 12 2009.

[Khu18] N. Khumalo and M. Mathuthu. Determination of trace elements and lanthanide (ree) signatures in uranium mine products in south africa by means of inductively coupled plasma mass spectrometry. *Journal of Geochemical Exploration*, 186:235-242, 2018.

[Kim17] T.K. Kim. Understanding one-way anova using conceptual figures. *Korean journal of anesthesiology*, 70(1):22, 2017.

[Kin16] J. Kinnaird and P. Nex. Uranium in africa. *Episodes*, 39:335, 06 2016.

[Ko12] W. Ko and F. Gao. Economic analysis of different nuclear fuel cycle options. *Science and Technology of Nuclear Installations*, 2012, 2012.

[Kra14] J. Krajkó *et al.,* Application of neodymium isotope ratio measurements for the origin assessment of uranium ore concentrates. *Talanta*, 129:499-504, 2014.

[Kri04] M.J. Kristo *et al.,* Model action plan for nuclear forensics and nuclear attribution. *Lawrence Livermore National Laboratory.[2004]. URL: Https://ereports-Ext. Llnl. gov/pdf/305453.* Pdf (access Date: 15.01. 2010), 2004.

[Kri11] M.J. Kristo. Nuclear forensics in radiometric methods of detection. *Technical report, Lawrence Livermore National Lab.(LLNL), Livermore, CA (United States)*, 2011.

[Kri16] M.J. Kristo *et al.,* Nuclear forensic science: analysis of nuclear material out of regulatory control. *Annual Review of Earth and Planetary Sciences*, 44:555-579, 2016.

[L'An12] M.F. L'Annunziata. Handbook of radioactivity analysis. *Academic press*, 2012.

[Lil13] J. Lilley. Nuclear physics: principles and applications. *John Wiley & Sons*, 2013.

[Lin09] K.L. Linge and K.E. Jarvis. Quadrupole icp-ms: Introduction to instrumentation, measurement techniques and analytical capabilities. *Geostandards and geoanalytical research*, 33(4):445-467, 2009.

[Mal09] D. Maltoni *et al.,* Handbook of fingerprint recognition. *Springer Science & Business Media*, 2009.

[Mal11] M.C. Malley. Radioactivity: a history of a mysterious science. *Oxford University Press*, 2011.

[Mar12] A. Martin. An Introduction to Radiation Protection 6E. *CRC Press*, 2012.

[Mar19] B.R. Martin and G. Shaw. Nuclear and particle physics: an introduction. *John Wiley*, 2019.

[Mat17] M. Mathuthu and N. Khumalo. Developing nuclear forensics signatures and national nuclear forensics librariesfor the african continent: A case review for south africa. *International Journal of Applied Science - Research and Review*, 4(1):1-3, 2017. ISSN 2394-9988.

[Max13] O. Maxwel *et al.,* Comparison of activity concentration of ^{238}U, ^{232}Th and ^{40}K in different layers of subsurface structures in deidei and kubwa, abuja, northcentral Nigeria. *Radiation Physics and Chemistry*, 91:70-80, 2013.

[May07] K. Mayer *et al.,* Nuclear forensic science—from cradle to maturity. *Journal of Alloys and Compounds*, 444:50-56, 2007.

[May12] K. Mayer *et al.,* Nuclear forensic science: correlating measurable material parameters to the history of nuclear material. *Chemical Reviews*, 113(2):884-900, 2012.

[May13] K. Mayer *et al.,* Nuclear forensic science: Correlating measurable material parameters to the history of nuclear material. *Chemical Reviews*, 113(2):884-900, 2013. PMID: 23194287.

[Mis12] K.C. Misra. Introduction to geochemistry: principles and applications. *John Wiley & Sons*, 2012.

[Moo14] K.J. Moody *et al.,* Nuclear forensic analysis. *CRC Press*, 2014.

[Nas11] K.L. Nash and G.J. Lumetta. Advanced separation techniques for nuclear fuel reprocessing and radioactive waste treatment. *Elsevier*, 2011.

[Nic06] G. Nicolaou. Determination of the origin of unknown irradiated nuclear fuel. *Journal of environmental radioactivity*, 86(3):313-318, 2006.

[Oye18] T.D.T. Oyedotun. X-ray Fluorescence (XRF) in the investigation of the composition of earth materials: a review and an overview. *Geology, Ecology, and Landscapes*, 2(2):148-154, 2018.

[Par11] B.H. Park *et al.,* Comparative study of different nuclear fuel cycle options: Quantitative analysis on material flow. *Energy Policy*, 39(11):6916-6924, 2011.

[Peń16] M.V. Peńkin *et al.,* Application of uranium impurity data for material characterization in nuclear safeguards. *Journal of Radioanalytical and Nuclear Chemistry*, 307(3):1995-1999, 2016.

[Pir11] D. Pirrie and G.K. Rollinson. Unlocking the applications of automated mineral analysis. *Geology Today*, 27(6):226-235, 2011.

[Pro11] WISE Uranium Project. Uranium mining and milling wastes: An introduction, 2011. Accessed on 2019-05-13.

[Pro19] WISE Uranium Project. Integrated nuclear fuel cycle information systems, 2019. Accessed on 2019-02-13.

[Rea16] D.G. Reading. Nuclear forensics: determining the origin of uranium ores and uranium ore concentrates via radiological, elemental and isotopic signatures. *PhD thesis, University of Southampton*, 2016.

[Red09] A. Redermeier. Fingerprinting of nuclear material for nuclear forensics. *Esarda Bulletin*, 43:71-76, 2009.

[Rut10] E. Rutherford *et al.,* Radiations from radioactive substances. *Cambridge University Press*, 2010.

[Sch18] I.J. Schwerdt *et al.,* Nuclear proliferomics: A new field of study to identify signatures of nuclear materials as demonstrated on alpha-UO3. *Elsevier*, 186:433-444, 2018.

[Sha11] M.S. Shackley. An introduction to X-Ray Fluorescence (XRF) analysis in archaeology. In *X-ray Fluorescence spectrometry (XRF) in geoarchaeology*, pages 7-44. Springer, 2011.

[Sil13] P. Silvennoinen. Nuclear Fuel Cycle Optimization: Methods and Modelling Techniques. *Elsevier*, 2013.

[Sim13] A. Simonetti *et al.,* Nonproliferation and nuclear forensics: Detailed, multi-analytical investigation of trinitite post-detonation materials. *Mineralogical Association of Canada Short Course 43*, Winnipeg MB, May 2013, p. 1-5.

[Spa17] T.L. Spano *et al.,* A novel nuclear forensic tool involving deposit type normalized rare earth element signatures. *Terra Nova*, 29(5):294-305, 2017.

[Srn11] M.B. Srncik. Investigation of the ^{236}U occurrence in the environment. *PhD thesis, uniwien*, 2011.

[Sta13] F.E. Stanley *et al.,* A brief introduction to analytical methods in nuclear forensics. *Journal of Radioanalytical and Nuclear Chemistry*, 295(2):1385–1393, 2013.

[Šve08] J. Švedkauskaitė-Le Gore. Development and validation of a method for origin determination of uranium-bearing material, 2008.

[Swi15] M.W. Swinney. Experimental and Computational Assessment of Trace Nuclide Ratios in Weapons Grade Plutonium for Nuclear Forensics Analysis. *PhD thesis*, 2015.

[Var09] Z. Varga *et al.,* Application of lead and strontium isotope ratio measurements for the origin assessment of uranium ore concentrates. *Analytical Chemistry*, 81(20):8327-8334, 2009.

[Var17] Z. Varga *et al.,* Identification of uranium signatures relevant for nuclear safeguards and forensics. *Journal of Radioanalytical and Nuclear Chemistry*, 312(3):639-654, 2017.

[Vér10] A. Vértes *et al.,* Handbook of Nuclear Chemistry: Vol. 1: Basics of Nuclear Science. *Springer Science & Business Media*, 2010.

[Wal06] M. Wallenius *et al.,* Nuclear forensic investigations: two case studies. *Forensic science international*, 156 (1):55-62, 2006.

[Win17] F. Winde *et al.,* Uranium from africa-an overview on past and current mining activities: Re-appraising associated risks and

chances in a global context. *Journal of African Earth Sciences*, 129:759-778, 2017.

[Wu12] C. Wu *et al.,* How reliable is X-Ray Fluorescence (XRF) measurement for different metals in soil contamination? *Environmental Forensics*, 13(2):110-121, 2012.

[Zhu17] M. Zhuang *et al.,* Concentrations and health risk assessment of rare earth elements in vegetables from mining area in shandong, china. *Chemosphere*, 168:578-582, 2017.